ESTIMATION OF SOURCE ROCK POTENTIAL OF THE SEMBAR FORMATION BY INTEGRATION OF WELL LOGS AND WELL CUTTINGS DATA IN THE SOUTHERN INDUS BASIN, PAKISTAN

A thesis submitted to Bahria University, Islamabad in partial fulfillment of the requirement for the degree of M.S in Geology

HAROON AZIZ

Department of Earth and Environmental Sciences

Bahria University, Islamabad

2017

ABSTRACT

The Sembar Formation encountered in Khajari-01 and Miran-01 wells are located in the Sanghar-south district Sindh, and Gupchani Block of Nawabshah District, Sindh, Pakistan. The crucial indicator for evaluation of source rock potential is total organic carbon (TOC) content. TOC is generally measured by traditional methods like evaluation of side wall cores, well cuttings or cores in geochemical lab. Data obtained from these experimental techniques are not continuous and time-consuming process. A solution to this problem is high resolution and continuous information from well logs. Different methods were used to estimate TOC through well logs. Out of these methods, four methods have been chosen to estimate TOC, i.e Schmoker and Hester, Fertl and Chilingar, Passey, and Multivariate fitting method. These estimated values have been correlated with well cuttings TOC values to optimize a method for TOC estimation through well logs. Fourteen well cuttings samples of Sembar Formation from well Khajari-01 and seven samples from Miran-01 well have been evaluated for geochemical parameters, because every well logs TOC estimation method is restricted to some specific environments. These parameters were used for evaluation of the formation to determine the quality, quantity and maturity of organic matter.

Van krevelen diagram of HI verses OI and Langford diagram of S2 verses TOC indicate that Sembar Formation of Khajari-01 well contain kerogen type-III which is gas prone, while that of Miran-01 contain Kerogen type-IV, which is non-productive. TOC indicate the organic richness in Khajari-01 well as poor to very good and in Miran-01 fair to good, while S2 indicate poor potential yield in both wells. Maturity indicators i.e Tmax and Production Index show an immature to early mature zone for Khajari-01 well and over mature zone for Miran-01 in the Sembar Formation. Natural gamma-ray spectroscopy method has poor correlation coefficient values with cuttings tested TOC with R^2 values of 0.1446 for well Khajari-01 and 0.2359 for well Miran-01. Schmoker and Hester method also gives poor R^2 values of 0.2878 and 0.5828. Multivariate fitting method has also poor correlation coefficient values of 0.3556 and 0.0333. Passey method was best fitting method with high R^2 values of 0.8018 for well Khajari-01 and 0.8306 for well Miran-01.

ACKNOWLEDGMENTS

I would like to express my deepest gratitude and appreciation to my Supervisor, Dr. Muhsan Ehsan for his sincere help, continuous guidance and precious remarks throughout the reaearch work. I extend my heartily thanks to my teacher, Dr. Samina Jahandad, whose encouragement and support enabled me to develop better understanding of the subject.

My unlimited thanks should go to Oil and Gas development Company Limited, Islamabad for using the geochemistry lab. I am very much thankful to Directorate General of Petroleum Concession (DGPC) and LMKR, Islamabad for providing me the required data for this research. Dr. M. Saeed Khan Jadoon and Mr. Javed Iqbal Chaudry from Oil and Gas Development Company Limited (OGDCL) are thanked for their moral and technical support. I am grateful to the technical staff of Oil and Gas Development Company Limited (OGDCL) & teaching staff of Bahria University, for their help and assistance during my stay.

I am also very much thankful to my friends and classmates for fruitful discussions during this research. Last, but not the least, I am deeply thankful to my mother and father whose unconditional love and support always encouraged me to bring this research to a reasonable conclusion.

CONTENTS

CHAPTER 2

GEOLOGY AND TECTONICS

CHAPTER 3

STRATIGRAPHY OF THE STUDY AREA

CHAPTER 4

SOURCE ROCK POTENTIAL

CHAPTER 5

ESTIMATION OF TOC THROUGH WELL LOGS

CHAPTER 6

CORRELATION

FIGURES

Page

TABLES

Page

CHAPTER 1

INTRODUCTION

1.1. Introduction to study area

The largest onshore sedimentary Basin of Pakistan is Indus Basin having a total area of about 138,000 square kilometers. The targeted area for the study is the Southern Indus Basin of Pakistan which is geologically a complex area having different parts, i-e Sindh Monocline, Thar Platform, Kirthar Fold Belt, and Karachi Trough. The Southern Indus Basin is separated from the Central Indus Basin by the Jacobabad high and Mari-Kandhkot high located in the north of Southern Indus Basin, to the west there is Axial Belt, to the east, Indian Shield and to the south is Arabian Sea (Sheikh and Giao, 2017). Previously, it has been interpreted that Southern Indus Basin is an extensional basin, formed by the ancient rifting (Wandrey et al., 2004).

Sembar Formation of Lower Cretaceous age is confirmed as the primary source rock for most of the petroleum discoveries in the Southern Indus Basin, which is mainly shale, but minor lithologies of sandstone, siltstone, and limestone are also present (Zaigham and Mallick, 2000; Aadil et al., 2014). The Sembar Formation has total thickness of 133m at the type outcrop section at Sembar pass that the Sembar Formation is named after, 262m in the Moghal Kot outcrop section (Bender and Raza, 1995) and has a thickness of 760 to 1000 m in the subsurface of Southern Indus Basin (Zaigham and Mallick, 2000). The Sembar Formation thins toward the southeast of Southern Indus Basin. The age of the Sembar Formation has been defined by the Belemnite biostratigraphy which is mainly Neocambian (Lower Cretaceous) (Fatmi, 1977).

The exploration and production (E & P) of hydrocarbons are very much significant and essential for the economy and growth of a country. The US Energy Information Administration (EIA, 2013) published in its report about estimated shale oil and gas for some basins of Pakistan, but in-depth and comprehensive evaluation of shale oil and gas potential in Pakistan is required yet.

In the developing countries geologists are facing problems while doing research on shale oil and gas due to lack of geochemical data such as Total Organic Carbon Content (TOC), Hydrogen Index (HI), Oxygen Index (OI), Level of Maturity

Index (LMI), Tmax, S1, S2, Vitrinite Reflectance (R_o), and Level of Organic Maturity (LOM). Rock-Eval Pyrolysis and wells core samples of these geochemical parameters are very much expensive and time-consuming. Many researchers are trying to give the best possible solution to this problem by estimating these parameters from well logs.

There are different methods of TOC estimation from the well logs data, but sometimes there are a little bit differences while applying these methods. The purpose of the study is to propose the integrated methodology for the TOC estimation from the well logs data when the Rock-Eval data is not available.

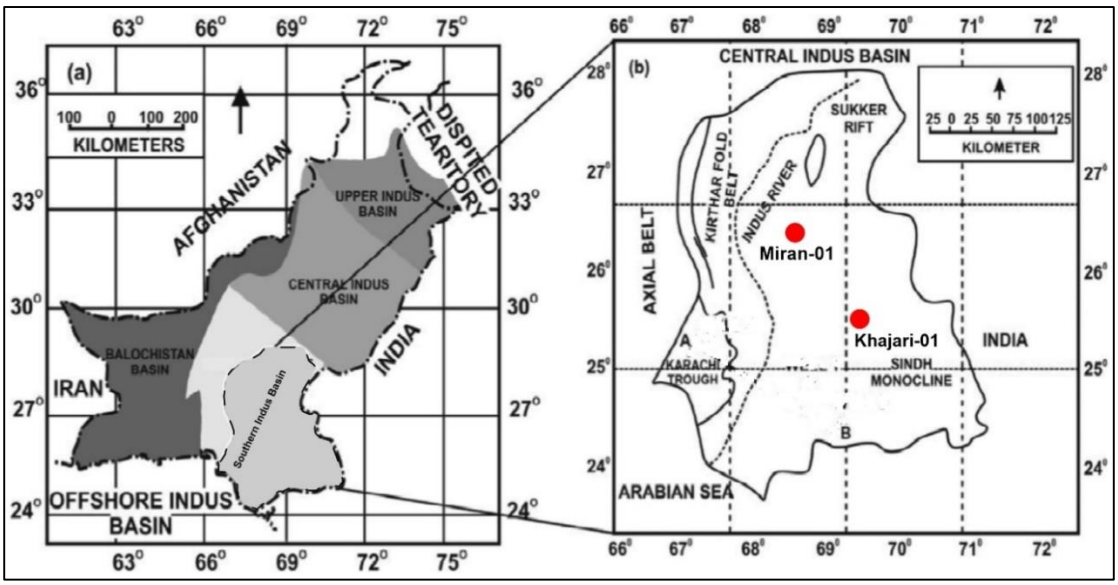

Figure 1.1 Location Map of Southern Indus Basin (Sheikh and Giao, 2017).

1.2 Objectives

The objectives of the research work are,

I) To determine the organic matter quantity, quality and maturity of Sembar Formation in Khajari-01 and Miran-01 wells.

II) To provide a better understanding to estimate the Total Organic Carbon (TOC) content by different methods with the use of well logs.

III) Comparison of TOC estimation methods and investigation for most reliable well log based TOC estimation for the Sembar Formation.

1.3 Data used

Table 1.1 Data used for achieving the objectives of the research are listed below, acquired from DGPC and OGDCL.

S.No.	Wells Name	Data Type	Lat and Long
1	Khajari-01	Digital LAS File – Sonic, Density, Neutron, Gamma Ray and Resistivity logs, Caliper, PEF (Photoelectric factor). TOC and Rock-Eval pyrolysis data	25° 27' 25.21'' N 69° 29' 08.36'' E
2	Miran-01	Digital LAS File – Sonic, Density, Neutron, Gamma Ray and Resistivity logs, Caliper, PEF (Photoelectric factor). TOC and Rock-Eval pyrolysis data	26° 23' 01.78'' N 68° 33' 17.9'' E

1.4 Source of data

Complete suites of well logs data were collected from LMKR after the preior permission of Directorate General of Petroleum Concession (DGPC), Pakistan. Rock-Eval data were collected by collection of well cuttings from Oil and Gas Development Company Limited (OGDCL) and then analysis of samples at OGDCL geochemistry lab.

1.5 Methodology

After collection of wells data from LMKR, the software Geographix is to be used for logs analysis.

Las files and well tops will be loaded into software which will give us complete suites of logs. From these logs, different methods will be used to estimate TOC.

1.5.1 Direct method of Total Organic Carbon (TOC) content measurement

Well cuttings samples of Sembar Formation from Khajari-01 and Miran-01 wells have been first prepared for processing in the C/S Analyzer CS-580A. These samples have been pulverized, sieved, acidified to remove carbonate minerals, and

neutralized. After the process of samples preparation, these samples were then subjected to C/S Analyzer CS-580A for total organic carbon (TOC) content measurement.

1.5.2 Rock-Eval pyrolysis

Samples preparation process for Rock-Eval pyrolysis is same as that of TOC measurement. After samples preparation the Rock-Eval Analyzer has been calibrated by applying the standard samples in geochemical lab. The prepared samples were then subjected to the analyzer to perform the process of Rock-Eval pyrolysis. Rock-Eval pyrolysis analyzer produce a pyrogram which show geochemical parameters, S1, S2, S3, and Tmax. The remaining parameters like generation potential (GP), production index (PI), oxygen index (OI), and hydrogen index can be calculated from the above parameters.

1.5.3 Indirect methods of Total Organic Carbon (TOC) content estimation

The following methods have been chosen for estimation of total organic carbon (TOC) content using well logs.

1.5.3.1 Natural Gamma-Ray Spectroscopy method (Schmoker et al., 1981)

Schmoker in 1981 introduced a method for TOC estimation through gamma-ray log in Appalachian Devonian shales. He described that organic matter is mostly associated with high values of gamma-ray activity. The empirical formula of TOC estimation through gamma-ray spectroscopy is,

$$phgr = \frac{(ggr_B - ggr)}{1.378A}$$

Where phgr is the organic matter content of the shale, ggr is the intensity of gamma-ray log measured in API unit, ggr_B is the intensity of gamma-ray, when organic matter is not present, and A is the slope of cross plot between intensity of gamma-ray log and formation density. The factors ggr_B and A are varying factors which can be measured regionally with the use of gamma-ray and density logs.

1.5.3.2 Schmoker and Hester (1983) Method

Schmoker and Hester calculated TOC values from formation density logs using the following equation.

$$TOC(Wt.\%) = \frac{154.497}{\rho b} - 57.261$$

Where TOC is total organic carbon content (Wt. %) and ρ_b is bulk density (g/cm^3) value of a formation.

1.5.3.3 Fertl and Chilingar, 1988 Method

Spectral gamma-ray logs measure the uranium content directly. This method is better than NGR spectroscopy, because other radioactive elements like potassium and thorium could not affect its results. The empirical formula for TOC calculation from uranium content presented by Renchun et al., 2015 in Upper Ordovician Wufeng Formation is,

$$TOC_{U} = 0.2381 \times a(w) + 0.2016$$

Where TOC_U is total organic carbon (TOC) content calculated from uranium log curve and a(w) is the uranium log curve values.

1.5.3.4 Passey et al., (1990) Method

Passey used the following empirical equation for calculating TOC in source rocks from ΔlogR:

$$TOC = \Delta \log R \times 10^{(2.297 - 0.168 \times LOM)}$$

Where ΔlogR is the curve separation between sonic, density, or porosity logs, and resistivity log and LOM is the amount of level of organic metamorphism.

The algebraic expressions that were used by Passey for the calculation of ΔlogR from the sonic/resistivity is:

$$\Delta \log R_{\Delta t} = \log_{10} R / R_{baseline} + 0.02(\Delta t - \Delta t_{baseline})$$

Where R is the resistivity measured in Ω m; Δt is the transit time measured in us/m; $R_{baseline}$ is the resistivity corresponding to the $\Delta t_{baseline}$ when the curves are baseline in nonsource rocks.

$$\Delta \log R\rho = \log_{10} R / R_{baseline} - 2.5(\Delta\rho - \Delta\rho_{baseline})$$

Where ΔlogRρ is separation value of resistivity/density crossover $\rho_{baseline}$ is baseline value of density.

$$\Delta \log R\varnothing = \log_{10} R / R_{baseline} + 4.0(\Delta\varnothing - \Delta\varnothing_{baseline})$$

Where ΔlogRØ is separation of resistivity and porosity, Ø $_{baseline}$ is baseline porosity value baseline interval.

$$\Delta \log R = \frac{\Delta \log R_{\Delta t} + \Delta \log R_{\Delta\rho} + \Delta \log R_{\Delta\varnothing}}{3}$$

ΔlogR is the average value of log curve separation between sonic, density, or porosity logs and resistivity log curve.

1.5.3.5 Multivariate fitting method

Multivariate fitting method was proposed by Renchun et al, in 2015. He proposed an equation which is based on bulk density of the formation, i-e density curve and the uranium curve in well log suits. The equation for multivariate fitting method is,

$$TOC_{MV} = 0.049 \times w(U) + (-13.373)(\rho b) + 36.735$$

Where TOC_{MV} is total organic carbon (TOC) content calculated from multivariate fitting method, w (u) is the uranium curve values and ρb is the density log curve values.

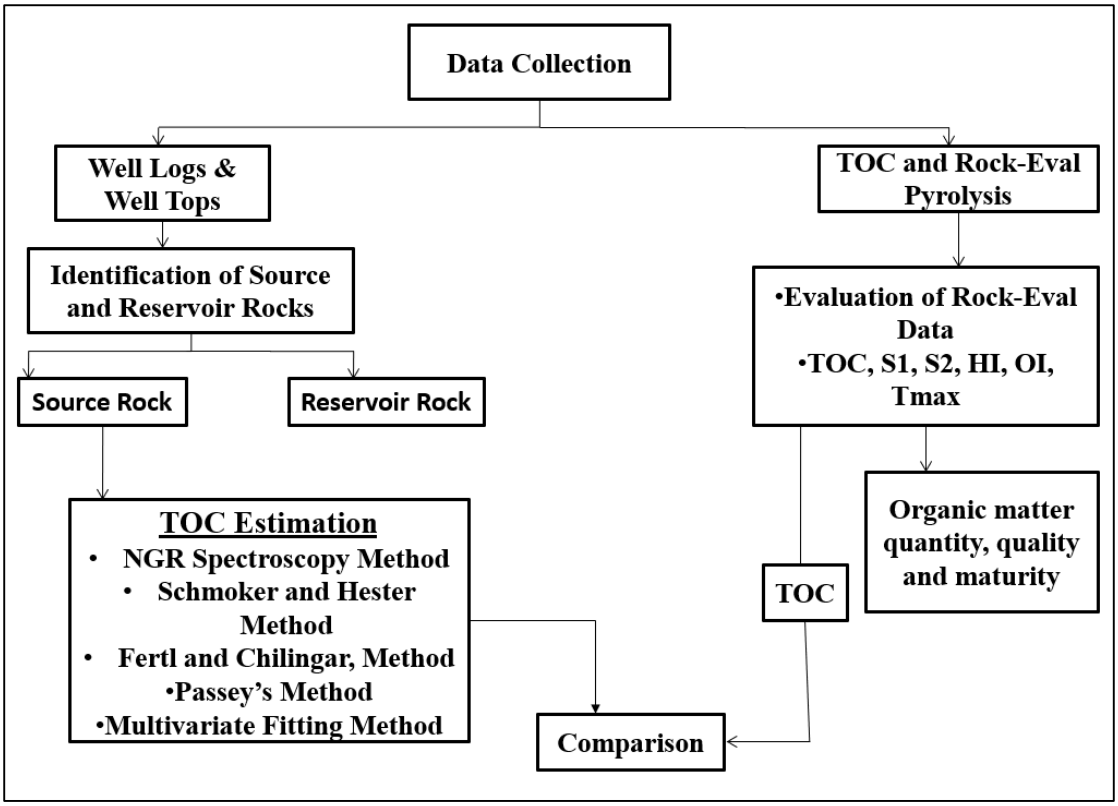

Figure 1.2 Flow chart of methodology followed in the research.

CHAPTER 2

GEOLOGY AND TECTONICS

2.1 General geology and tectonics

The thick shelf margin reefal limestone, which is originated in the Permo-Triassic age (Searle et al., 1983), represent the foremost rifting occurred of the Gondwanaland and origin of continental margin of Atlantic type. The initial rifting of the micro-continents away from the northern margin of the Gondwanaland can be discussed with the origin of Paleo-Neotethys with a spreading ridge in between (Stocklin, 1997). The micro plates were drifting slowly in the direction of north and later on in Cretaceous to Paleocene time welded with the Eurasian Plate. Indian Plate which was rifting from African Plate and Madagascar possibly initiated in Cretaceous time. This rifting started the regressive deposition of Early Cretaceous deltaic and associated deep sea of Fan lobes, which prograded throughout centeral and eastern Pakistan. The Early drift of the Indian Plate toward the north from Early to Middle Eocene was fast ranging from 130 to 150 m/y (Powell, 1979). Indian Plate which was moving counter clock wise relative to that of Eurasian Plate about a close pole at the time of Early Eocene was coincident and its velocity decreased to about 40 to 60 mm/y (Sclater and Fisher, 1974). This velocity of the Indian Plate finally got stable to 2 mm/y between Early Oligocene to present. At last collision of the Indian and Eurasian plates happened in Late Eocene. The mountain ranges of Himalayas have been originated due to the constant thrusting of Indian Plate beneath the Eurasian Plate since Cretaceous age (Patriat and Achache, 1984).

In the current plate tectonic settings, Pakistan lies on the northwest corner of the Indian lithosphere Plate which represent the part of tertiary convergence between the Indian and Eurasian Plates. Northern collision zone has been recognized as Indus-Tsangpo Suture (TS), Main Central Thrust (MCT), Main Boundary Thrust (MBT), and Main Frontal Thrust (MFT) (Gansser, 1981). The collision zone in northern Pakistan has been subdivided as the Main Karakoram Thrust (MKT) and Salt Range Thrust (SRT) (Farah et al., 1984; Yeasts and Lawrence, 1984).

Precambrian basement rocks are exposed along the Sargodha High about 80 km south of SRT. Its east-south east trend parallel to main Himalayas corresponds

Indian Plate and loading of south verging thrust sheets (Molnar et al., 1975; Duroy et al., 1989).

The collision in the west along a transpressional fault zone, the discontinuous belt of Ophiolites which run through Bela and Zhob valleys represent structure. Currently the Chaman/Ornach-Transform Fault Zone (COTFZ) represent the western boundary. The triple junction situated north-west of Karachi which is the eastern edge of the Makran Subduction Complex. The Indian Plate is separated from African Plate along the Carlsberge Ridge while the Owen Fracture Zone marks the boundary between the Indian and Arabian Plates.

The Middle Tertiary collision zone east of the COTFZ can be further divided into stratigraphically and tectonically different regions i.e Northern Mountain area, Axial Belt, and Indus Basin. Indus Basin is further divided into Upper, Middle, and Lower Indus Basins. The area west and northwest of the Axial Belt represent Balochistan Basin, which comprises Makran Subduction Complex and Kakar Khurasan Flysch Trough (Kemal., 1992).

The Lower Indus Basin represents progradational Mesozoic sequence on a westward inclined gentle slope. Every prograding time unit represent lateral facies variations from continental and shallow marine in the east to dominantly basinal to the west. In Thar slope region, all Mesozoic sediments are regionally plunging to the west and are truncated by unconformable volcanics and sediments of Paleocene time (Kemal, 1992).

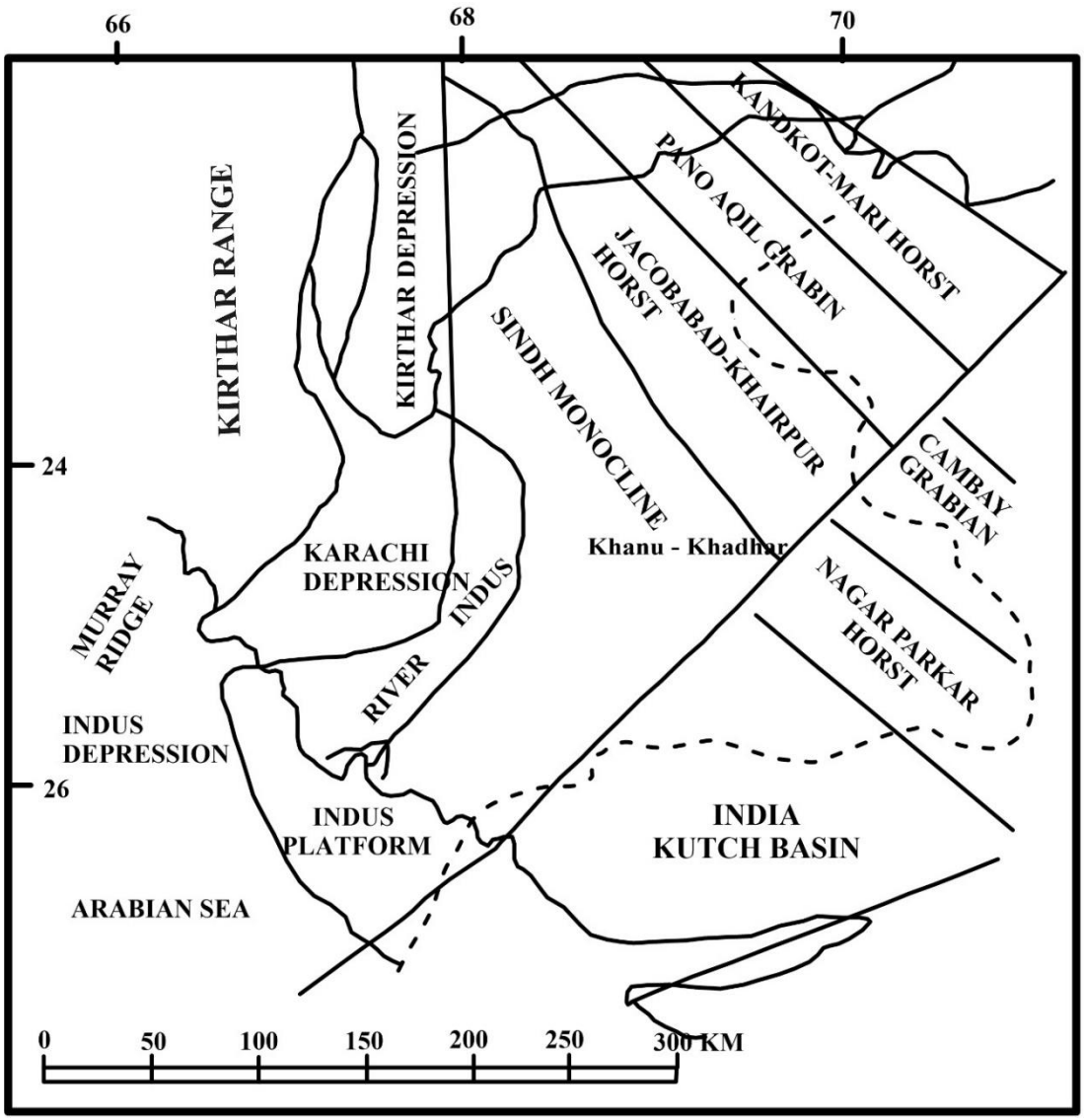

Figure 2.1 Tectonic map of Lower Southern Indus Basin (Modified after Raza et al., 1990).

2.2 Geology and tectonics of the study area

The whole Lower Indus Basin shows extensional tectonics, that is why, Normal Faults have been originated showing horst and graben structure with former being of great exploratory significance.

Offshore Indus in proximity and parallel to 67^{o} E longitude is separated into platform and depression along a hinge line. Offshore platform is separated by a line dividing Karachi trough from Thar slope onshore into Karachi trough and Thar deltaic zone platform offshore (Raza et al., 1990).

Lower Indus Basin is bounded by the Indian Shield to the east and the marginal zone of Indian Plate to the west. Its southward extension is confined by Offshore Murray Ridge. Owen Fracture plate boundary (Kadri, 1995). The platform and trough extend into the Offshore Indus. Lower Indus Basin contain Thar platform, Karachi depression/trough, Kirthar foredeep, Kirthar fold belt, Offshore Indus.

2.2.1 Thar platform

Thar platform is gently sloping monocline similar to Punjab Platform controlled by basement topography. The sedimentary wedge thins toward the Indian Shield whose surface expression are existing in the form of Nagar Parker High. It represents the buried structure originated due to extensional tectonics resulting from latest counter-clockwise drive of the Indian Plate. The platform represents very good development of Cretaceous sands (Goru) which are the producing reservoirs of oil/gas fields. Sindh monocline structure lies in the southeastern part of Thar platform (Kadri, 1995).

2.2.2 Karachi depression

Karachi depression is characterized by thick Early Cretaceous sediments and represents the last phases of marine sedimentation. It is comprised of several narrow chain-like anticlines, some of which contain gas fields. The Early, Middle, and Late Cretaceous rocks are well preserved in the area. The most interesting feature is the continuous deposition throughout the Cretaceous/Tertiary (K/T) boundary (Kadri, 1995).

2.2.3 Kirthar foredeep

Kirthar foredeep trends north-south and has received the sediments aggregating a thickness of over 15,000 meters. It has a faulted eastern boundary with Thar platform. The Upper Cretaceous is absent but Paleocene is well developed. This area has high potential for maturation of source rock (Kadri, 1995).

2.2.4 Kirthar Fold Belt

This north-south trending tectonic feature is similar to Sulaiman Fold Belt in structural style and stratigraphic correspondence. Rocks from Triassic to Recent were deposited in this region. The formation of Kirthar fold belt also represents the closing of Oligocene-Miocene seas (Kadri, 1995).

2.2.5 Offshore Indus

This area forms part of passive continental margin and seems to have gone through two different stages of geological history (Cretaceous-Eocene and Oligocene-Recent). Sedimentation in Offshore Indus area initiated from Cretaceous age (Kadri, 1995). Murray Ridge is the main tectonic structure formed in the Offshore Indus.

CHAPTER 3

STRATIGRAPHY OF THE STUDY AREA

The oldest formation in the Southern Indus Basin is Wulgai Formation of Triassic age which has a conformable contact with Shirinab Formation of Jurassic age by overlain Chiltan Limestone. In the Southern Indus Basin, the regional erosion occurred, and the Sembar and the Goru formations overlay the erosive surface. Throughout the late Cretaceous the shelf environment was continued, resulting in the deposition of the regressive sandstones of the Pab Formation in the west (Wandrey et al., 2004).

Lower Cretaceous includes Sembar and Goru formations, while the Late Cretaceous formations are Parh, Mughal Kot, and Pab. The outcrop of the Paleocene Ranikot Formation and Eocene Laki and Kirthar formations are mostly present onshore, whereas the Oligocene Nari Formation and the Miocene Gaj Formation are present offshore (Sheikh and Giao, 2017).

3.1 Shirinab Formation

The earliest Jurassic rock unit exposed in Lower Indus Basin is Shirinab Formation. It varies in thickness from about 1500 m to 3000 m (Fatmi, 1977). Lithology of Shirinab Formation contains interbedded limestone and shale. The Early Jurassic Shirinab Formation is mostly exposed in Loralai Districts of Baluchistan, Queta, Kalat and Zhob (Williams, 1959). This Formation is disconformably overlain by Sembar Formation of Lower Cretaceous age or Goru Formation of Lower Cretaceous age (Kazmi and Jan, 1997).

3.2 Chiltan Limestone

The lithology of middle Jurassic Chiltan Limestone contain chert and mainly limestone, which is massive to thick bedded having light grey to dark color and oolitic. It varies in thickness from 750 m to 1800 m and overlies the Shirinab Formation as gradational and conformable contact. This Formation is mostly exposed

in Quetta, Kalat, Sibi and Loralai District (Fatmi, 1977). Chiltan Limestone in the Lower Indus Basin is acting as a productive reservoir (Wandrey et al., 2004).

3.3 Sembar Formation

Most Early Cretaceous sequence of Lower Indus Basin contains black shale and siltstone with argillaceous limestone of Sembar Formation. Type localities of Sembar Formation are Sembar Pass and Mughal Kot section where its thickness are 133 m and 262 m respectively. Sembar Formation is overlain by Lower Goru Formation which shows gradational contact with each other, but unconformity is also reported at some places (Williams, 1959). Environmental condition under which the Sembar Formation is formed seems to be open-marine environment. The Sembar Formation present in the Lower and Middle Indus Basin is mostly considered as a source rock (Raza et al., 1990). Somewhere Sembar is also acting as reservoir (Wandrey et al., 2004).

3.4 Goru Formation

Goru Formation of Early Cretaceous age in the Lower Indus Basin is composed of sandstone, shale with interbedded marl, limestone and siltstone. Mostly the sandstone of Lower Goru Formation in the Lower Indus Basin has produced oil while the same sandstone in the Middle Indus Basin is one of the successful gas reservoirs (Nazir, 2013). Goru Formation in its type locality is reported as about 536 m and its environment of deposition varies from continental, transitional, deltaic, shallow marine to deep marine. Fauna reported are belemnite and forams (Shah, 1977).

Upper contact with Sembar Formation and lower contact with Parh Formation are both conformable. The top of Lower Goru member is an unconformable surface (Mozaffar et al., 2002). Goru Formation is divided into two members as, Upper Goru and Lower Goru members. Both the upper and lower members of Goru Formation are dominated by limestone. Variation in lithologies from claystone and sandstone toward limestone and marl is described by Lower Goru member while lithology variation from marl toward claystone is described by Upper Goru member. Shales of Goru

Formation are considered as source rock while sandstones are the main reservoir (Wandrey et al., 2004).

Table 3.1 Stratigraphic Succession of Lower Southern Indus Basin (Modified after Sheikh and Giao, 2017).

AGE				DESCRIPTION	LITHOLOGY
ERA	PERIOD	EPOCH	FORMATION		
CENOZOIC	QUARTERNARY	RECENT	ALLUVIUM	CLAY, SHALE, SANDSTONE, CONGLOMERATE	
		PLOCENE-PLESTOCENE	SIWALIK	SANDSTONE, SHALE, CONGLOMERATE	
	TERTIARY	MIOCENE	GAJ	SHALE, LIMESTONE, SANDSTONE	
		OLIGOCENE	NARI		
		EOCENE LATE			
		EOCENE MIDDLE	KIRTHAR	SHALE, LIMESTONE	
		EOCENE EARLY	LAKI	LIMESTONE INTERBEDDED SHALE	
		PALEOCENE	RANIKOT	LIMESTONE, SANDSTONE, SHALE, BASALT	
MESOZOIC	CRETACEOUS	LATE	PAB	SANDSTONE, SHALE	
			MUGHAL KOT	LIMESTONE, SHALE WITH MINOR SANDSTONE	
			PARH	LIMESTONE	
		MIDDLE	GORU UPPER	MARLY SHALE	
			GORU LOWER	SANDYSHALE	
		EARLY	SEMBAR	OIL/GAS SHALE	
	JURASSIC	LATE			
		MIDDLE	CHILTAN	LIMESTONE	

3.5 Parh Limestone

The Late Cretaceous Parh Limestone is composed of thin to medium bedded limestone with subordinate marl intercalations and calcareous shale. Both the upper and lower contacts with Mughalkot and Upper Goru formations are conformable. Its

type locality is Parh Range. Thickness of Parh Limestone is variable in different areas from 300 m to 600 m but in type locality, thickness is 268 m. Parh Limestone in the Southern Indus Basin is acting as a reservoir (Shah, 1977).

Table 3.2 Borehole stratigraphy of wells, Khajari-01 and Miran-01.

Age	Formation	Formation tops (m)	Thickness (m)
Well Miran-01			
Recent	Alluvium	0.00	518.00
Eocene	Kirthar	518.00	146.00
Eocene	Laki	664.00	630.00
Paleocene	Ranikot	1,294.00	645.00
Paleocene	Khadro	1,939.00	126.00
Late Cret/early cret	Parh	2,065.00	175.00
Late Cret/Early Cret	Upper Goru	2240.00	235.00
Early Cretaceous	Lower Goru	2475.00	1631.00
Early Cretaceous	Sembar	4106.00	98.00
Middle Jurassic	Chiltan	4204.00	196.00
Well Khajari-01			
Recent	Alluvium	0	437
Eocene	Laki	437	178
Paleocene	Ranikot	615	54
Early Cretaceous	Lower Goru	669	1,054
Early Cretaceous	Sembar	1,723	586
Middle Jurassic	Chiltan	2,309	812
Early Jurassic	Shirinab	3,121	379

3.6 Khadro Formation

Lithology of Paleocene Khadro Formation contains brown, olive, green to grey, medium grained and soft sandstone and olive gypsiferous and grey to brown shale which is interbedded with fossiliferous limestone. It also contains basaltic lava flows and is distributed in the vast area of Kirthar and its adjacent areas. Environment of deposition of Khadro Formation is marine (Kazmi and Jan, 1997). Type locality of

Khadro Formation is Bara Nai in Lakhi Range. Formation thickness is about 60 to 180 m in different places. Lower contact of the formation with Pab Formation is reported as unconformable while its upper contact with Ranikot Formation is conformable (Kazmi and Jan, 1997).

3.7 Ranikot Formation

The upper part of Early Paleocene Ranikot Formation is composed of grey limestone with shale and brown sandstone while the lower part comprised of sandstone with limestone and shale interbeds. Its environment of deposition is shallow marine. Lower contact of Ranikot Formation with Khadro Formation is unconformable while its upper contact with Laki Formation is conformable (Kazmi and Jan, 1997). Sandstones and limestones of Ranikot Formation are the proven reservoir rocks in the Southern Lower Indus Basin (Wandrey et al., 2004).

3.8 Laki Formation

Laki Formation of Early Eocene age is composed of cream to grey colored limestone with subordinate calcareous shale, sandstone, marl and laterite. Environment of deposition of Laki Formation is shallow marine. Type locality of Laki Formation is in northern Lakhi Range near Mari Nai. It is mainly exposed in the southern Sulaiman Range and southern Kirthar Range lower contact of Laki Formation with Ranikot Formation is unconformable while its upper contact with Ghazij Formation is conformable (Kazmi and Jan, 1997).

3.9 Kirthar Formation

Lithology of middle Eocene Kirthar Formation mainly consist of fossiliferous limestone interbedded with subordinate marl and shale. Limestone of the formation is massive to thick bedded and nodular. Its environment of deposition is shallow marine. Upper contact of Kirthar Formation with Siwaliks is disconformable while its lower contact with Ghazij Formation is conformable (Shah et al., 1977). Kirthar Formation in the Lower Indus Basin is considered as a productive reservoir rock (Wandrey et al., 2004).

3.10 Siwaliks

Siwaliks are the recently Pleistocene age deposited material. Lithology of Siwaliks is characterized by the cyclic deposition of clastic origin clays and sandstone. Environment of deposition of Siwaliks is continental fluvial (Shah, 1977).

3.11 Alluvium

Alluvium is a general term used for gravel, sand silt, clay or unconsolidated detrital material which have been deposited in a recent geological time through a medium like stream, or running water, as semi-sorted or sorted sediments. This type of materials is typically deposited in the bottom of a river which form floodplains and deltas. These materials may be deposited at any spot where river joins a lake or run-offs its boundaries (Kazmi and Jan, 1997).

CHAPTER 4

SOURCE ROCK POTENTIAL

4.1 Geochemical screening

Geochemical testing of formation cuttings, sidewall cores, conventional cores from well, and outcrop samples can help to determine the amount, type, and maturity of organic matter. It helps geoscientists to determine whether, how much, when, and where petroleum might have been generated and what secondary processes might have been occurred after expulsion of petroleum from source rock. The process of geochemical studies is shown in the figure 4.1.

4.1.1 Source rock screening

A fine-grained rock which is rich in organic matter, which is subjected to enough temperature and pressure has the potential to generate hydrocarbons is a source rock (Tissot and Welte, 1984; Hunt, 1996). According to Hunt (1996), capacity of generation of petroleum is describe by quality and quantity of source rock. Others like Peters, 1986 and Spiro, 1991 reported Rock-Eval Pyrolysis as the most reliable and accepted technique for source rock evaluation. Total of 14 samples of Sembar Formation from Khajari-01 well and 7 samples from Miran-01 well were used for this study.

The quality of source rock is evaluated to check for:

I. Organic richness (TOC)
II. Hydrocarbon potential (pyrolysis S1 & S2)
III. Kerogen type (Pyrolysis & maceral analysis)
IV. Thermal analysis (Pyrolysis-T_{max} and Rock-Eval calculated PI)

These parameters help to differentiate potential source rock from poor one.

Identification of thermally mature source rock is landmark achievement for exploration.

4.2 Sample preparation for determination of Total Organic Carbon (TOC)

Well cuttings samples were collected from OGDCL as core samples were not available after the prior permission of OGDCL authority. These samples were first examined physically to remove any contamination, if present and to conform the lithology. After the pre-examination, the samples have been washed to remove the unwanted mud and impurities. These samples have been dried on a hot plate at about 130 ^{o}C and pulverized using mortar and pestle, so that it can pass through 60µ sieve.

4.2.1 Total Organic Carbon (TOC) as a screening tool

A pulverized and sieved sample of about 500 mg weighed on electronic balance was taken in a beaker as shown in figure 4.1.

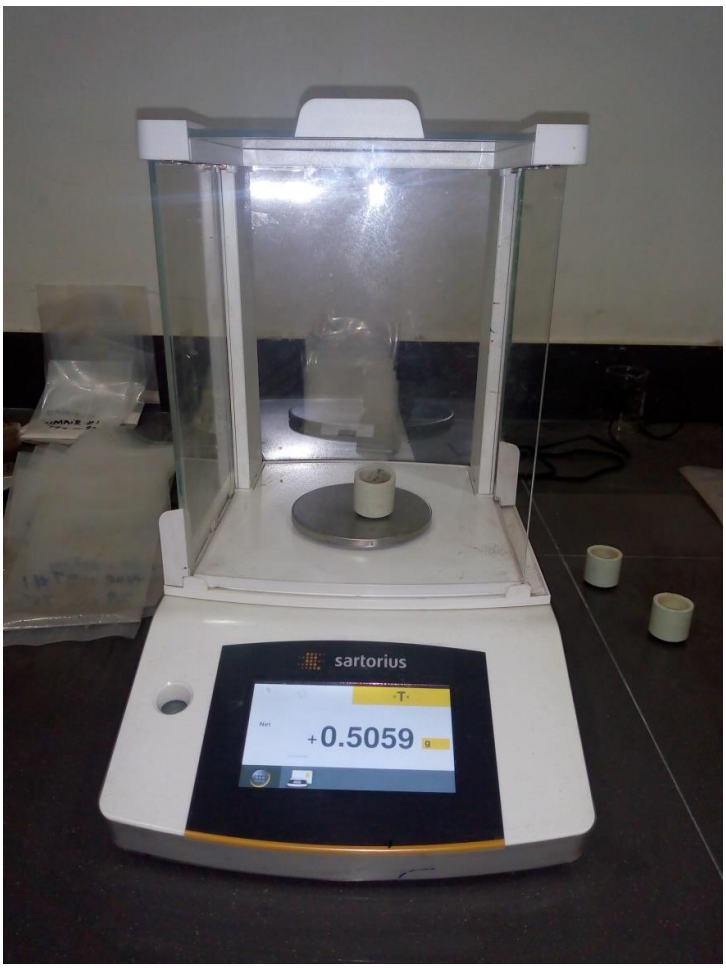

Figure 4.1 Electronic balance used to weigh a pulverized sample.

4.2.1.1 Acidification

Sedimentary rocks contain carbonate minerals as cementing materials which are not required at the time of TOC determination. These carbonate minerals can be removed using HCL. 10% v/v HCL solution has been used to remove the carbonate minerals. Quantity of acid used was as much, until the reaction in the sample gets stopped, so that the carbonates could be removed completely. The sample was then dried on a hot plate at about 100 ^{o}C for further process.

Figure 4.2 10 % HCL used to remove the carbonate minerals.


Figure 4.3 Hot plate used to dry samples analyzed.

4.2.1.2 Neutralization using automatic titration

After acidification, samples need to be neutralized. The samples were then cooled and automatic titrator of SCHOTT Company was used for neutralization. Sodium hydroxide solution (NAOH) was used for the process of neutralization. The titrator adds solution automatically to the beaker having the sample, unless the PH value becomes 7. It stops adding further solution, once the solvent become neutralized completely. After the process of neutralization, the samples were dried once again on a hot plate at about 100 ^{o}C.

4.3 Analysis

Samples were transferred to ultra 580 crucibles from the beakers when dried completely. These samples in the crucibles were now ready for autoloading to analyze Total Organic Carbon (TOC) in the C/S-Analyzer auto-sampler.

Figure 4.4 Automatic titrator used for neutralization of samples.

4.3.1 Procedure of ELTRA Carbon/Sulfur Analyzer CS-580A

A gripper picks the crucibles and places it on pedestal one by one into the furnace for process of combustion. It takes minimum 60 and maximum 120 second for analysis. Signals of detector and other parameters of the instrument are shown during analysis. Also, overall evaluation and display of the signals are done automatically. The final data could then be transferred to Laboratory Information System (LIMS) software for further interpretation.

Carbon/Sulfur Analyzer gives values in the form of weight percentage (wt %). These values could then be plotted on different cross plots against Rock-Eval data for further interpretation.

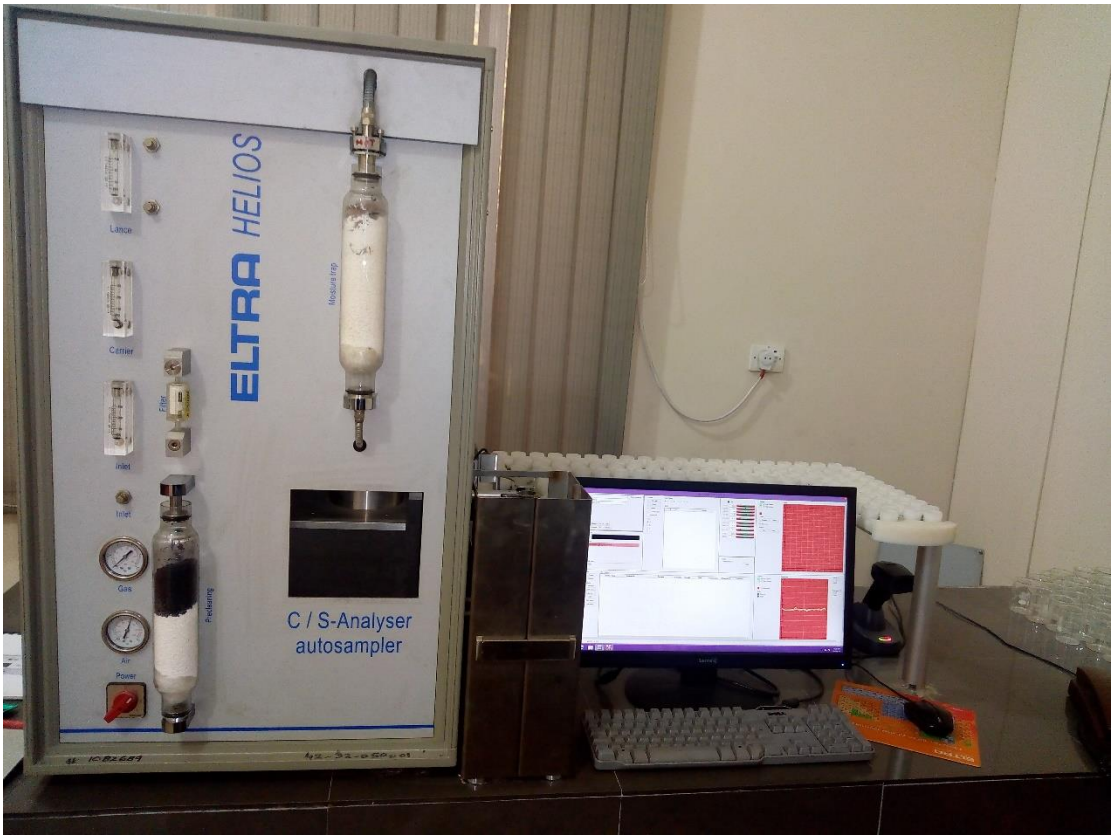

Figure 4.5 Carbon/Sulfur Analyzer CS-580A.

Table 4.1. Source rock potential expressed as wt % (Peters and Cassa, 1994).

Potential (Quantity)	TOC (Wt. %)
Poor	< 0.5
Fair	0.5 – 1
Good	1 – 2
Very Good	2 – 4
Excellent	> 4

4.4 Rock-Eval Pyrolysis

Sample preparation for Rock-Eval pyrolysis is same as that of the TOC determination. In case of delay between sample preparation and running pyrolysis, suitable conditions should be provided to the samples, i-e freezing conditions for reservoir rocks and anoxic conditions for kerogens.

4.4.1 Calibration

The Rock-Eval Analyzer has been calibrated with standard sample before running analysis of the required samples. First, two crucibles, one empty and the other with a standard sample processed in the instrument. Then the standard sample's Rock-Eval parameters have been verified with accepted standard parameters values. The process of calibration is for the reason to know, whether the instrument is working properly or not. A blank crucible has been run with analysis of the required samples. Every cycle of the analysis should contain this blank crucible, so that the analysis could be protected from ambiguity. Rock-Eval parameters obtained from the blank crucible have automatically stored in a blank repertory. Blank line has been automatically subtracted from all analysis.

4.4.2 Loading samples/Running samples

Crucibles for loading samples generally have a volume of 0.12 cubic centimeter. Keep in mind that crucibles used for calibration should be representative of the set of crucibles used for analysis. 70 mg of prepared samples from each selected depth samples have been weighed in crucibles using electronic balance. These crucibles have then loaded into the autosampler using nipper.

Now using computer screen, 'setup' of the Analyzer has been opened. All the samples have been analyzed one by one by selecting one at a time. Data of each sample could be automatically saved in database, but folder should be selected for saving data at first time.

Rock-Eval pyrolysis of each sample obtains a pyrogram, from which the following parameters could be analyzed.

S1: Free hydrocarbon in the rock sample which vaporized at up to 300 ^{o}C. It is measured in milligram of hydrocarbons per gram of a rock sample (mg HC/g R).

S2: Remaining potential of a rock to generate hydrocarbons by thermal cracking of kerogens at temperature up to 300-600 ^{o}C. It is also measured in milligram of hydrocarbons per gram of a rock sample (mg HC/g R).

Table 4.2 Source Rock evaluation criteria based on Rock-Eval parameters (Peters and Cassa, 1994).

Quality	**S1**	S2
Poor	0-0.5	0-2.50
Fair	0.5-1	2.50-5
Good	1-2	5-10
Very Good	2+	10+

S3: Amount of organic carbon dioxide, which evolves between 300-390 ^{o}C. it is measured in milligram of CO_2 per gram of a rock sample (mg CO_2/g R).

Hydrogen Index (HI): Relative hydrogen content in a rock sample. It can be calculated from S2 and TOC as,

$$HI = (S2 \times 100)/TOC$$

Table 4.3 Geochemical parameters showing petroleum potential of source rock (Peters and Cassa, 1994).

Kerogen (Quality)	**Hydrocarbon type**	**Hydrogen index**
I	Gas	50-200
II	Oil and Gas	200-300
II/III	Oil	300-600
IV	Oil	>600

Oxygen Index (OI): Relative oxygen content in a rock sample. It can be calculated from S3 and TOC as,

$$OI = (S3 \times 100)/TOC$$

Tmax: The temperature at which maximum S2 hydrocarbons evolves. It is measured in Degree Celsius (^{o}C).

Production Index (PI): The ratio of S1 to S1+S2. It can be calculated from S1 and S2 as,

$$PI = [S1/ (S1 + S2)] \times 100$$

Table 4.4 Thermal maturity stages (Peters and Cassa, 1994 and Bacon et al., 2000).

Stages of thermal maturity		**Tmax for Type-I**	**Tmax for Type-II**	**Tmax for Type-III**	**Production Index (PI)**
Immature		<440	<435	<445	<0.10
Mature	Early	440	435	445	0.10-0.25
	Peak	445	440	450	0.25-0.40
	Late	450	460	470	>0.40
Post Mature		>450	>460	>470	-

Generation Potential (GP): Total quantity of hydrocarbons present in a rock sample, which means, S1+S2. It represents the bulk potential of a rock sample to generate hydrocarbons. It is also measured in milligram of hydrocarbons per gram of a rock sample (Peters and Cassa, 1994).

$$GP = S1 + S2$$

Table 4.5 TOC and Rock-Eval data of Sembar Formation, Khajari-01 well.

S.No.	Depth (m)	Fm	TOC Wt %	S1 mg/g	S2 mg/g	S3 $mgCO_2/g$	T_{max} ^oC	GP Kg/ton	PI	OI	HI
1	1980-82	Sembar	0.39	0.39	1.12	1.08	417	1.51	0.26	277	287
2	1990-92	Sembar	0.39	0.56	0.45	0.49	419	1.01	0.55	126	115
3	2000-02	Sembar	1.42	0.73	1.01	1.03	419	1.74	0.42	73	71
4	2010-12	Sembar	1.37	0.34	0.62	0.79	419	0.96	0.35	58	45
5	2020-22	Sembar	2.16	0.62	1.12	1.17	427	1.74	0.36	54	52
6	2030-32	Sembar	1.05	0.92	0.90	0.82	428	1.82	0.51	78	86
7	2040-42	Sembar	1.80	1.01	1.06	1.15	429	2.07	0.49	64	59
8	2052-54	Sembar	1.42	0.95	2.30	1.48	429	3.25	0.29	104	162
9	2062-64	Sembar	1.53	0.90	0.53	0.72	431	1.43	0.63	47	35
10	2072-74	Sembar	1.21	1.09	1.29	1.41	432	2.38	0.46	117	107
11	2084-86	Sembar	0.82	1.06	0.92	0.97	432	1.98	0.54	118	112
12	2094-96	Sembar	0.64	0.92	0.62	0.71	430	1.54	0.60	111	97
13	2104-06	Sembar	0.98	0.90	0.78	0.65	433	1.68	0.54	66	80
14	2112-14	Sembar	0.79	1.18	0.45	0.52	418	1.63	0.72	66	57

Table 4.6 TOC and Rock-Eval data of Miran-01 well.

S.No.	Depth (m)	Fm	TOC Wt %	S1 mg/g	S2 mg/g	S3 mgco2/g	T_{max} °C	GP Kg/ton	PI	OI	HI
1	4110-12	Sembar	0.90	0.17	0.11	0.16	478	0.28	0.61	18	12
2	4120-22	Sembar	0.99	0.17	0.11	0.14	478	0.28	0.61	14	11
3	4140-42	Sembar	1.19	0.25	0.39	0.37	476	0.64	0.39	31	33
4	4160-62	Sembar	1.65	0.17	0.62	0.59	481	0.79	0.22	36	38
5	4170-72	Sembar	1.35	0.56	0.42	0.45	480	0.98	0.57	33	31
6	4190-92	Sembar	1.23	0.34	0.36	0.38	476	0.70	0.49	31	29
7	4200-02	Sembar	1.50	0.20	0.45	0.49	479	0.65	0.31	33	30

4.5 Organic matter quality

The quality of organic matter can be determined by plot of hydrogen index verses oxygen index (HI vs OI) and total organic carbon (TOC) content verses S2 values (TOC vs S2). These plots tell about the type of organic matter and original source input.

4.5.1 Type of Organic Matter

HI and OI is the representation of hydrogen and oxygen contents in the rock samples. HI and OI are indicators of origin of the organic matter. Hydrogen index is more reliable than oxygen index for determining the potential of a source rock to generate oil and gas. Formula for calculating Oxygen Index is (100 × S3)/TOC and that of Hydrogen Index is (100 × S2)/TOC (Tissot and Welte, 1984, Peters and Cassa, 1994 and Hunt, 1996). Calculated values for the wells, Khajari-01 and Miran-01 are given in tables 4.5 and 4.6. Samples of Sembar Formation from Khajari-01 well appear to have kerogen Type-III except three samples in which two samples are Type-IV and one II/III mixed, while samples of Sembar Formation from Miran-01 well appear to have kerogen Type-IV. Based on criteria defined by Peters and Cassa (Table 4.3), Sembar Formations of Khajari-01 has the potential to generate gas while Miran-01 well has none potential.

The value of hydrogen index is calculated from S2 (remaining potential), which mean, it does not give original value for samples. Although plot of HI verses OI is used to differentiate the organic input, either marine or terrestrial. The studied samples of Sembar Formation from wells Khajari-01 and Miran-01 both seems to be predominantly sourced by terrestrial input.

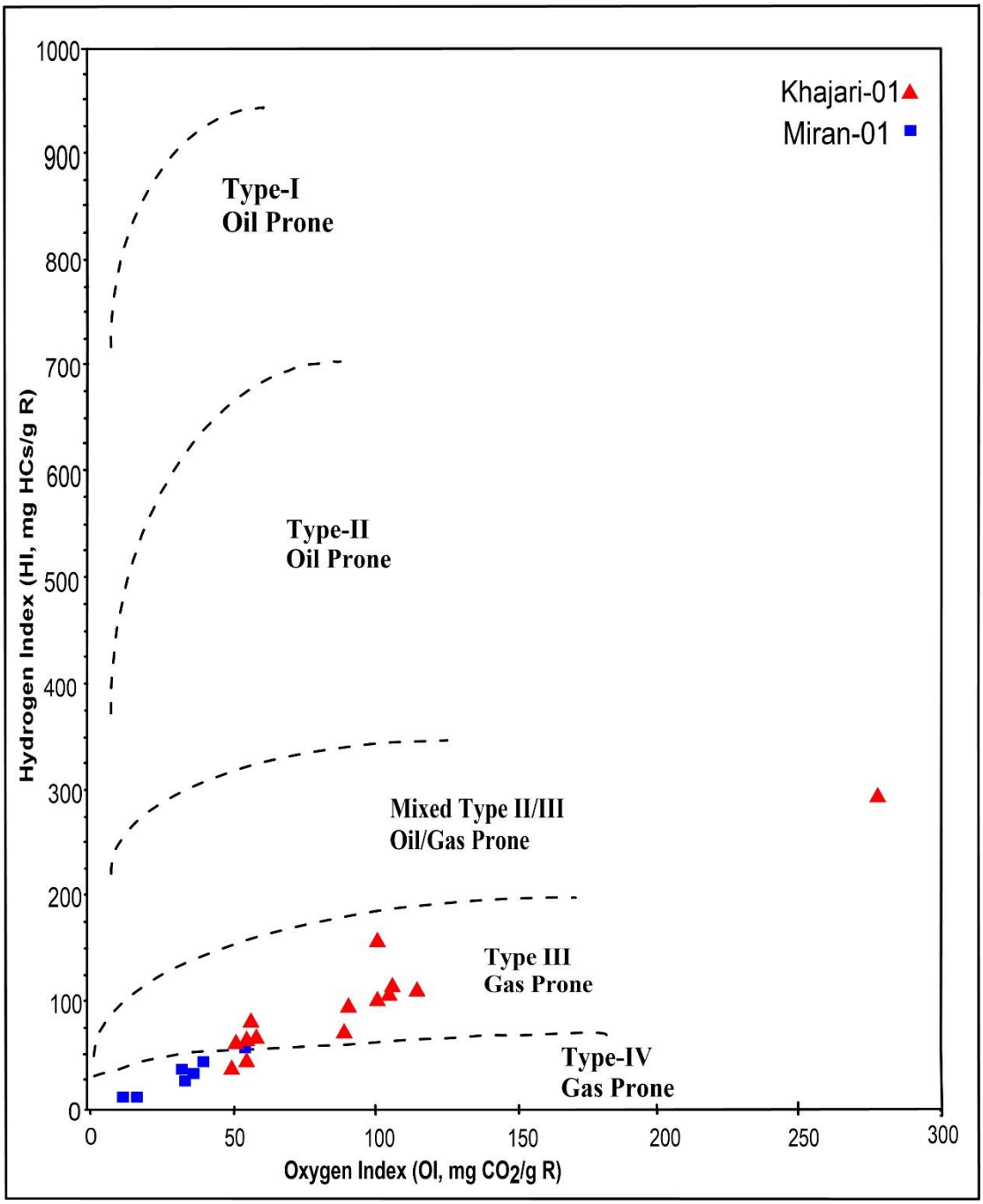

Figure 4.6 Cross plot of HI vs OI (modified Van Krevelen diagram) showing kerogen type of the selected samples.

4.5.2 TOC vs. S2

The plot of TOC verses S2 is used to determine the type of organic matter. Quality of kerogen can also be determined from TOC verses S2 cross plot. The most reliable plot for differentiating the type of organic matter is TOC verses S2, because there is no dubious oxygen effect. Plot of TOC verses S2 shows that samples of

Sembar Formation from khajari-01 well lies in kerogen type-III region which is gas prone except 2 samples in which one sample lie in type-IV region which is dry gas prone while the other in II/III mixed which is oil and gas mixed. Samples from Miran-01 well falls in the region of type-IV kerogen, which is non-productive.

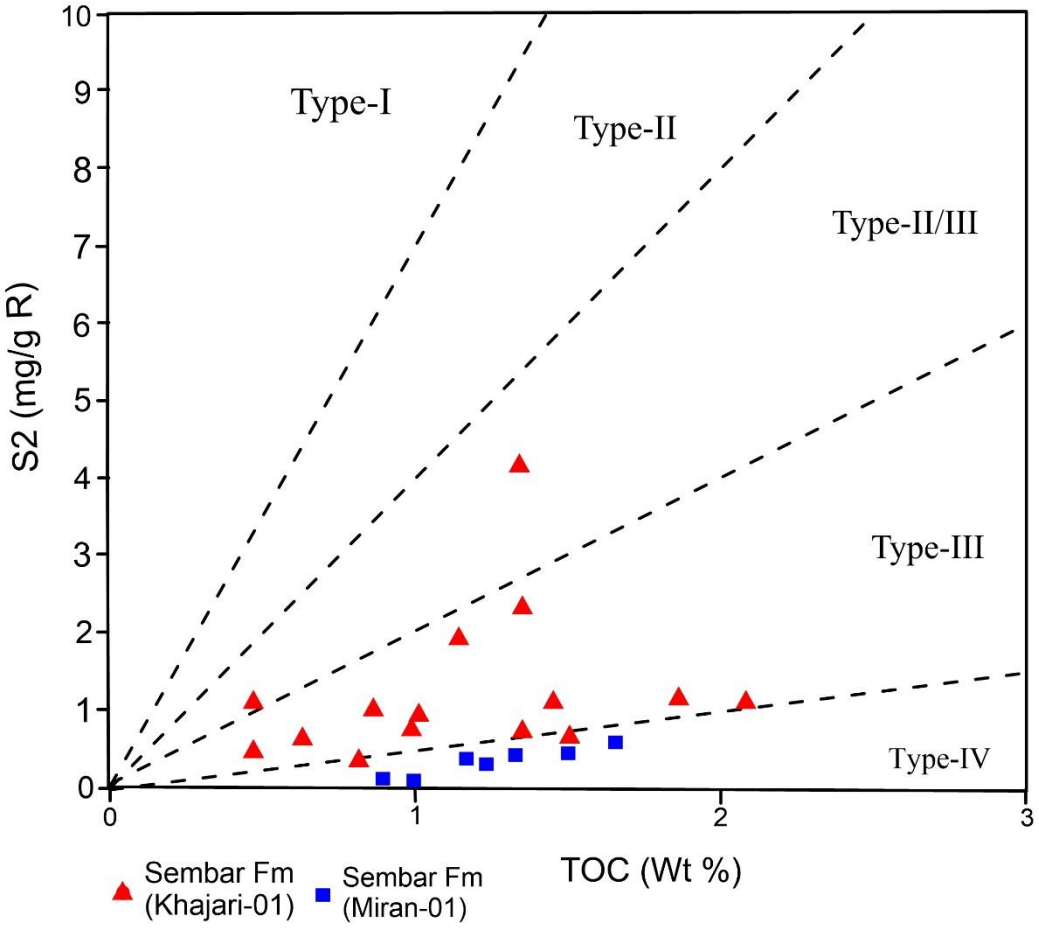

Figure 4.7 Diagram shows type of organic matter with petroleum prone (Langford and Blanc-Valleron, 1990).

4.6 Quantity of organic matter

Quality of organic matter can be determined from total organic carbon (TOC) content, S2 peak, and generation potential (GP). TOC indicate organic matter richness, S2 peak indicate petroleum potential and plot of generation potential (GP) verses TOC indicate the effectiveness of source rock.

4.6.1 Petroleum potential and organic richness

The petroleum potential and organic richness of the selected rock samples have been evaluated by total organic carbon (TOC), measured by C/S-Analyzer and the pyrolysis S2 peaks. As per the criteria defined by Peters and Cassa, the well khajari-01 falls in the category of poor to good, and one sample very good source rock, while the well Miran-01 shows fair to good source rocks in terms of organic richness. In terms of potential yield Khajari-01 well values variation in between 0.45-2.30 mg HCs/g which lies in the category of poor potential yield. Also, samples from Miran-01 well shows values in between 0.11-0.62 mg HCs/g which also lies in the category of poor potential yield.

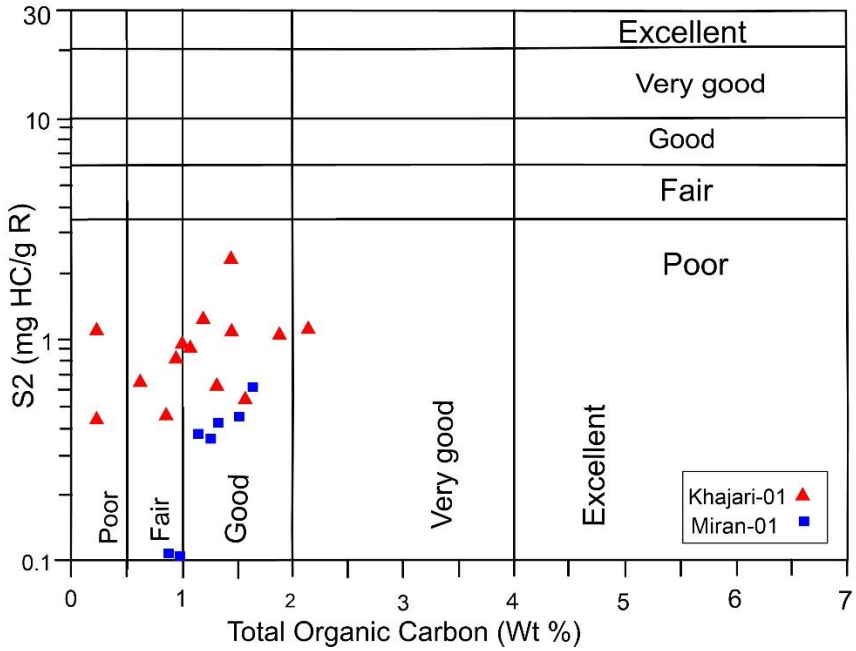

Figure 4.8 Cross plot of S2 verses TOC showing Hydrocarbon potential and organic richness.

4.6.2 Source rock characterization

The important information required in the initial exploration stages is the presence or absence of effective source rock. This information can be acquired from the plot of total organic carbon (TOC) verses generation potential (S1+S2) (Figure 4.10). Samples from the well khajari-01 falls in the category of poor to good source rock except one sample which is in the excellent region while samples from well Miran-01 lies in fair to good source rock as shown in the Figure 4.9.

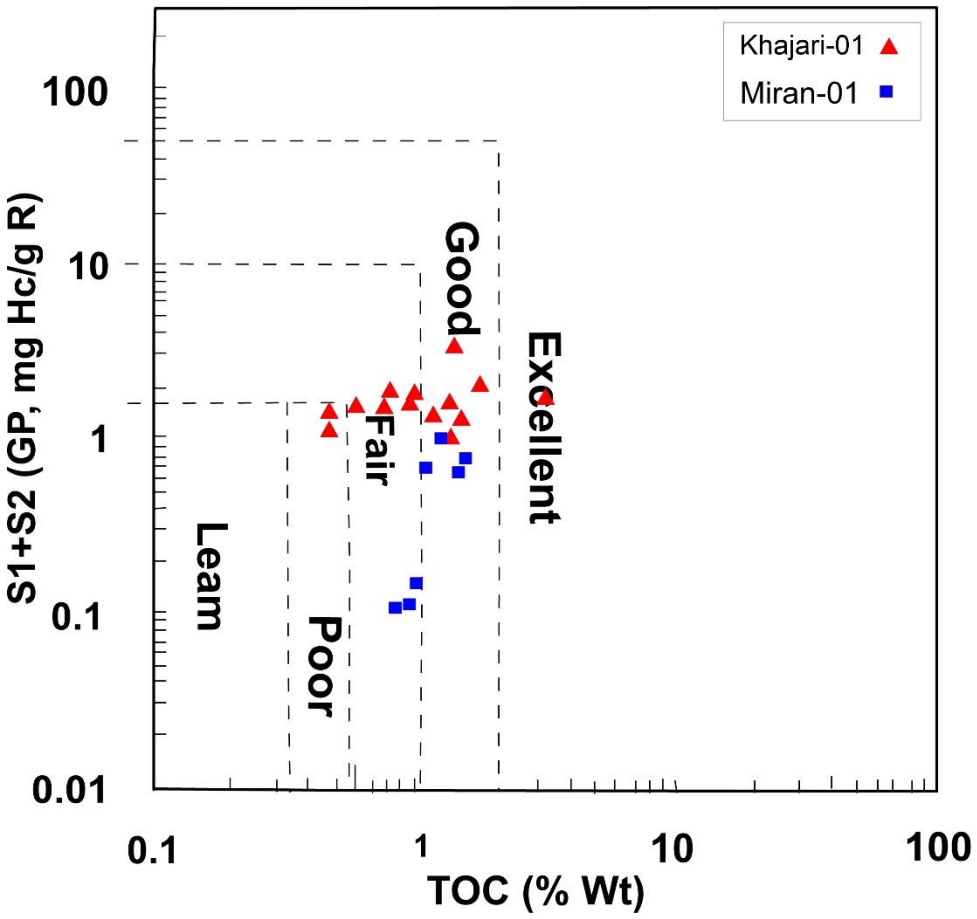

Figure 4.9 Cross plot of TOC verses GP showing quality of a source rock.

4.7 Maturity of organic matter

The level of thermal changes because of high temperature indicates maturity of source rock. Thermal maturity is affected by the amount of excess free hydrocarbons, i-e S1 and type of source rock organic matter along with other factors, i-e burial depth, burial age, and mineral matter.

Maturity level of organic matter increases as Tmax increases, which is due to the chemical reactions taking place during thermal cracking. Bonds which are weak breakup in the initial stages while stronger in the latter stages, having ability to survive in high temperatures.

The relationship between Production Index verses Tmax has been drawn as shown in the Figure 4.11 for detection of thermal maturity of organic matter. Based on the criteria defined by Peters and Cassa for Tmax and Production Index, samples from the well khajari-01 are immature, while sample from well Miran-01 well are

over mature. Production Index in the well Khajari-01 shows high values which are an indicator of high maturity. Here these high values of Production Index are due to the contamination in the sample. Samples of Sembar Formation from Khajari-01 well may have not properly washed before analysis, which is why it shows high values.

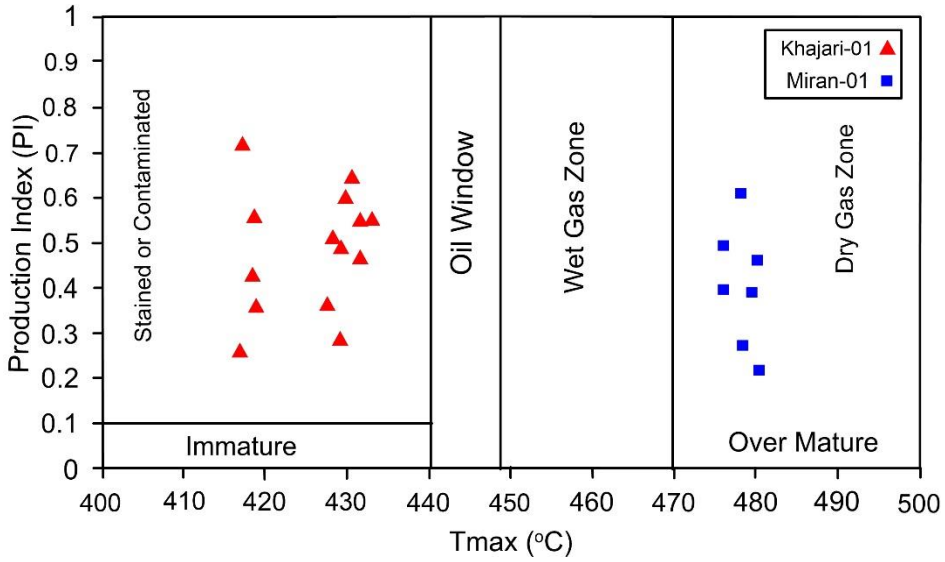

Figure 4.10 Cross plot of Production Index vs Tmax showing maturity levels.

CHAPTER 5

ESTIMATION OF TOC THROUGH WELL LOGS

The important indicator of evaluating shale oil and gas reservoir is the total organic carbon (TOC). TOC is generally measured by traditional methods like measuring TOC of side wall cores, well cuttings or cores in geochemical laboratory through source rock evaluation equipment. The data acquired from experimental methods are not continuous and time consuming. High resolution and continuous information though well logging can give a solution to the problems mentioned above.

As compare to the non-hydrocarbon source rock zone, shale oil and gas reservoir zones have a different response in well logs which is due to the unique physical properties of the organic matter. These properties of organic matter show high gamma-ray, high resistivity, high acoustic transit time and low-density properties. Different geoscientists around the world employed different techniques to estimate TOC from these well log's responses. The most popular methods among them for estimating TOC from these well log curves are,

i) Natural Gamma-Ray Spectroscopy method (Schmoker et al., 1981)
ii) Schmoker and Hester (1983) method
iii) Fertl and Chilingar, (1988) method
iv) Passey et al., (1990) method
v) Multivariate fitting Method (Johnson and Wichern, 2008)

5.1 Natural Gamma-Ray Spectroscopy method (Schmoker et al., 1981)

Schmoker in 1981 introduced a method for TOC estimation through gamma-ray log in Appalachian Devonian shales. He described that organic matter is mostly associated with high values of gamma-ray activity. He further explained that this high gamma-ray activity is due to the factors like, high uranium content of water at deposition time, organic matter type deposited, and sediment deposition rate. The empirical formula for TOC estimation through gamma-ray log developed by Schmoker is,

$$phgr = \frac{(ggr_B - ggr)}{1.378A}$$

Where phgr is the organic matter content of the shale, ggr is the intensity of gamma-ray log measured in API unit, ggr_B is the intensity of gamma-ray, when organic matter is not present, and A is the slope of cross plot between intensity of gamma-ray log and formation density. The factors ggr_B and A are varying factors which can be measured regionally with the use of gamma-ray and density logs.

Later, Schmoker realized that this method can only be used for the specific region of Appalachian Devonian shales, because gamma-ray log response is not for kerogen but uranium. The uranium content is also dependent on chemistry of water, type of kerogen and rate of sedimentation. So, one cannot assume exactly that either the high gamma-ray log response is associated with high TOC or not.

5.2 Schmoker and Hester, (1983) Method

Schmoker and Hester (1983) observed that there is an inverse relation between the formation rock density and total organic carbon (TOC), when he was doing research on carbonaceous shales of Assam Basin in India. Later, he introduced an empirical formula for estimating total organic carbon (TOC) from density log for Appalachian Devonian shales in United States. This empirical formula is given below.

$$TOC(Wt.\%) = \frac{154.497}{\rho b} - 57.261$$

Where TOC is total organic carbon and ρb is well logs values of bulk density of the formation.

Based on research of Appalachian shale of Devonian, Schmoker and Hester conformably proposed that there is an inverse relationship between TOC and formation rock bulk density. So, it possible in a similar manner to determine other shale gas reservoir through this relationship.

Schmoker's and Hester method is one of the easiest methods of TOC calculation, because there is only one well logging curve involved in calculation of TOC i-e bulk density log curve. In this research we also chose to calculate TOC of

Sembar Formation in the Lower Southern Indus Basin through Schmoker's and Hester method.

The algorithm of Schmoker and Hestler can estimate TOC in clay-poor shales which is thermally mature. Basically, this algorithm needs calibration with the lithotype. However, results may be ambiguous with either underestimation of TOC in clay-rich or carbonate rich shales or overestimation in thermally immature shales.

5.3 Fertl and Chilingar, (1988) Method

Spectral gamma-ray logs measure the uranium content directly. This method is better than NGR spectroscopy, because other radioactive elements like potassium and thorium could not affect its results. The empirical formula for TOC calculation from uranium content presented by Renchun et al., 2015 in Upper Ordovician Wufeng Formation is,

$$TOC_{U} = 0.2381 \times a(w) + 0.2016$$

Where TOC_U is total organic carbon (TOC) content calculated from uranium log curve and a(w) is the uranium log curve values.

There may still be errors because of the minerals which are uraniferous, like phosphates, which misguide while estimating TOC. Issues like sedimentation rate and water chemistry may also misguide while estimating TOC through Fertl and Chilingar, method.

5.4 Passey et al., (1990) Method

Passey et al, developed a practical technique called the ΔlogR technique for calculating and identifying total organic carbon (TOC) content in organic-rich rocks through well logs. He used the overlying of sonic, porosity, and density logs over the resistivity log, specifically the deep resistivity log.

The ΔlogR technique proposed by Passey has been used in many wells worldwide and has worked successfully. Later, other methods have also been introduced to the industry, like gamma-ray spectral logs which gives more advantages

of calculating organic content directly but Passey method has been successfully tested for calculation of TOC both in the clastic and carbonate source rocks.

He used the following empirical equation for calculating TOC in source rocks from ΔlogR technique.

$$TOC = \Delta \log R \times 10^{(2.297 - 0.168 \times LOM)}$$

Where ΔlogR is the curve separation between sonic, density, or porosity log curves, and resistivity log curve and LOM is the amount of level of organic metamorphism.

LOM can be found using Vitrinite Reflectance (R_o) values by the chart given in figure 5.5. The average value of R_o has been calculated for the well Khajari-01, which is 0.51, and that of Miran-01 is 1.45. The corresponding values of LOM against R_o values are 8.11 for the well Khajari-01 and 11.5 for well Miran-01.

The algebraic expression that was used by Passey for the calculation of ΔlogR from the sonic/resistivity is:

$$\Delta \log R_{\Delta t} = \log_{10} R / R_{baseline} + 0.02(\Delta t - \Delta t_{baseline})$$

Where R is the resistivity measured in Ω m; Δt is the transit time measured in us/m; Rbaseline is the resistivity corresponding to the Δtbaseline when the curves are baseline in non-source rocks.

Also, the expression that was used to calculate ΔlogR from density/resistivity curves is,

$$\Delta \log R\rho = \log_{10} R / R_{baseline} - 2.5(\Delta\rho - \Delta\rho_{baseline})$$

Where ΔlogRρ is separation value of resistivity/density crossover ρbaseline is baseline value of density.

$$\Delta \log R\varnothing = \log_{10} R / R_{baseline} + 4.0(\Delta\varnothing - \Delta\varnothing_{baseline})$$

Where ΔlogRØ is separation of resistivity and porosity, Ø baseline is baseline porosity value baseline interval.

Passey et al., (1990) pointed in his paper that ΔlogR method can give ambiguous values in the shales with very high maturity, i-e when LOM value is >10.5

and Vitrinite Reflectance values >0.9. Renchun et al., 2015 confirmed that for Jiaoshiba Shale gas reservoir R_o value from 2.42 to 3.12 %, there comes limitations of TOC estimation through ΔlogR method.

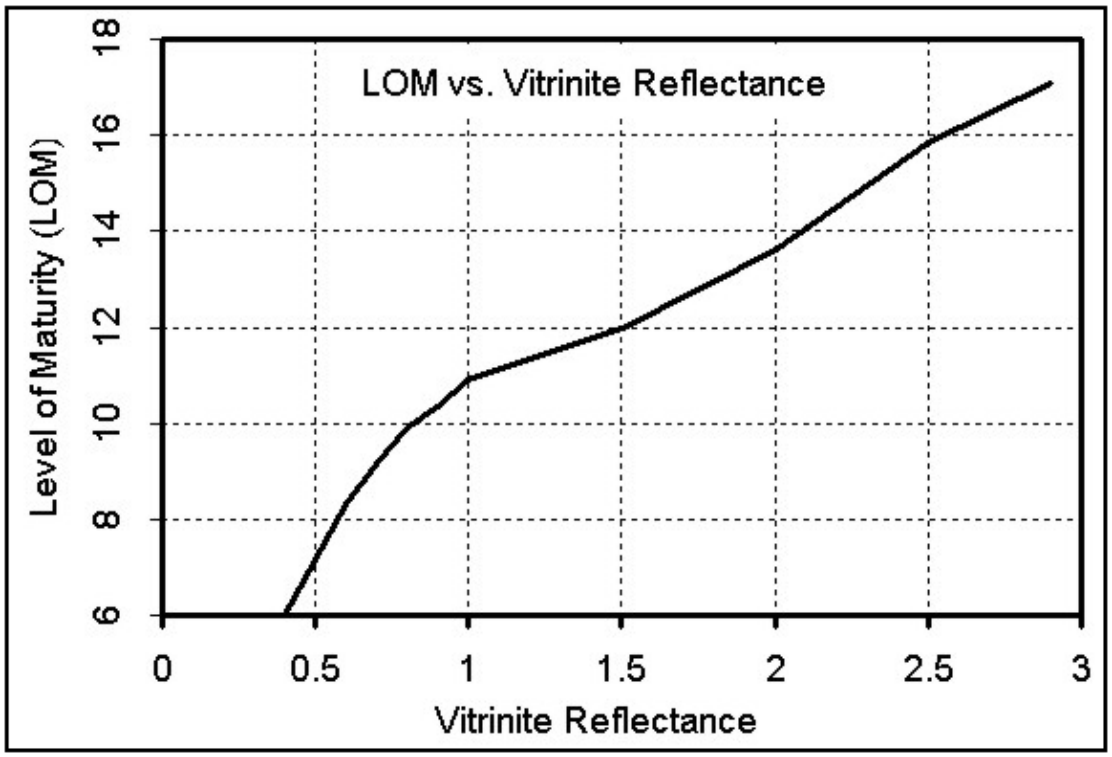

Figure 5.1 Graph for determining Level of organic maturity (LOM) from Vitrinite Reflectance (R_o) (Crain, 2006).

5.5 Multivariate fitting method

Multivariate fitting method has been established by Renchun et al, in 2015. He improved the equation of Schmoker et al, by adding another parameter of uranium content in the equation. As from the Schmoker's method we already know that, there is an inverse relation between the bulk density and total organic carbon (TOC) content of a formation. Uranium content in lithology of shale also increases with the presence of total organic carbon (TOC) content (Abshire et al, 2017). The multivariate fitting equation for calculation of total organic carbon is,

$$TOC_{MV} = 0.049 \times w(U) + (-13.373)(\rho b) + 36.735$$

Where TOC_{MV} is total organic carbon, w(U) is the uranium log curve value and ρ is the density log curve value.

Multivariate fitting method can be easily used to calculate TOC through uranium log curve and bulk density log curve in marine mud shale formation.

Table 5.1 Reliability of TOC estimation methods.

TOC Estimation Methods	**Reliability**	
	Khajari-01	**Miran-01**
NGR Spectroscopy	×	×
Schmoker and Hester Method	✓	✓
Fertl and Chilangar, (1988) Method	✓	✓
Passey et al., (1990) Method	✓	✓
Multivariate Fitting Method	✓	✓

Total organic carbon (TOC) content has been calculated by the above-mentioned methods. Figures 5.2, 5.3, 5.4, 5.5, and 5.6 shows the calculated TOC separately. Brown and blue curves show the overlay of sonic and deep resistivity logs. The separation between blue and brown is ΔlogR. Baseline for Sembar Formation in well Khajari-01 is taken as 2.018 ohm.m for resistivity curve and 85.863 us/ft for sonic log curve. In a similar way for well Miran-01, basline is taken as 7.39 ohm.m and 71.24 us/ft. The three green curves show the calculated TOC and the red small intervals shows the TOC measured from the samples in geochemical lab through Carbon/Sulfur analyzer.

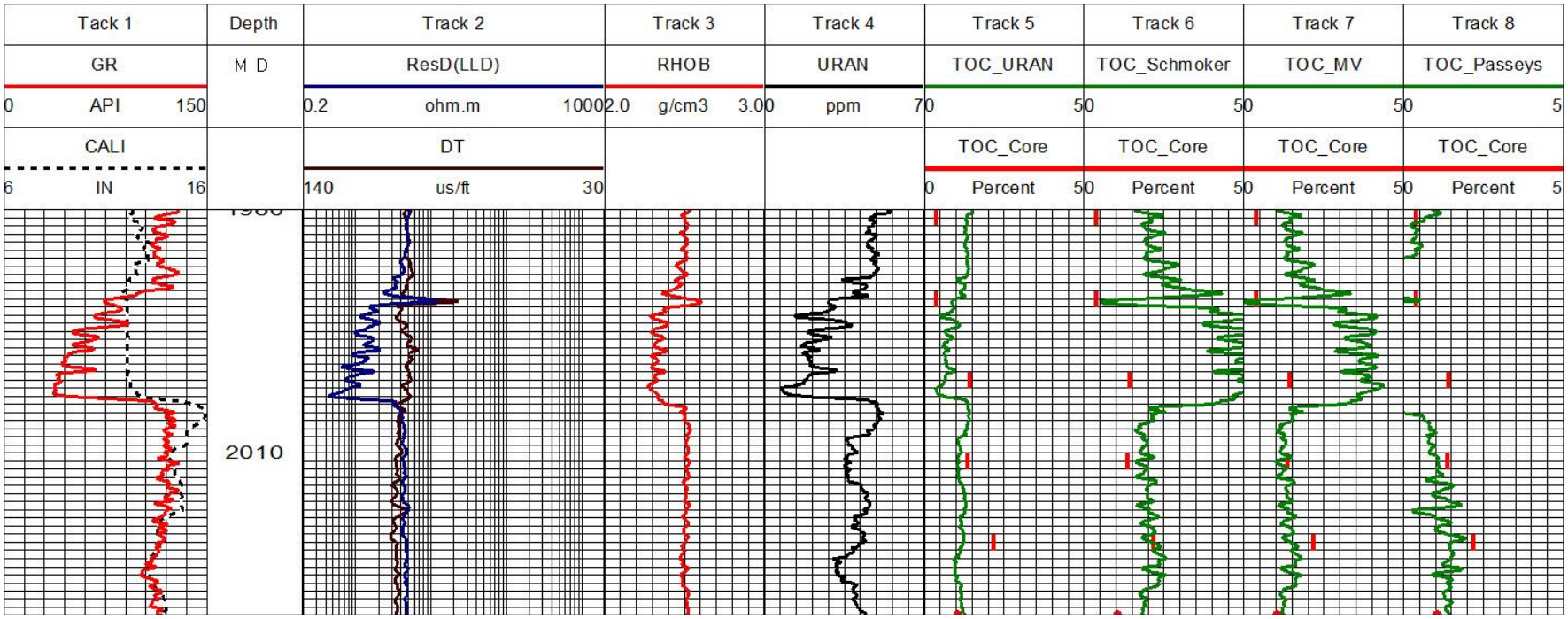

Figure 5.2 TOC estimation of Sembar Formation in Khajar-01 well through selected methods at a depth 1980-2030.

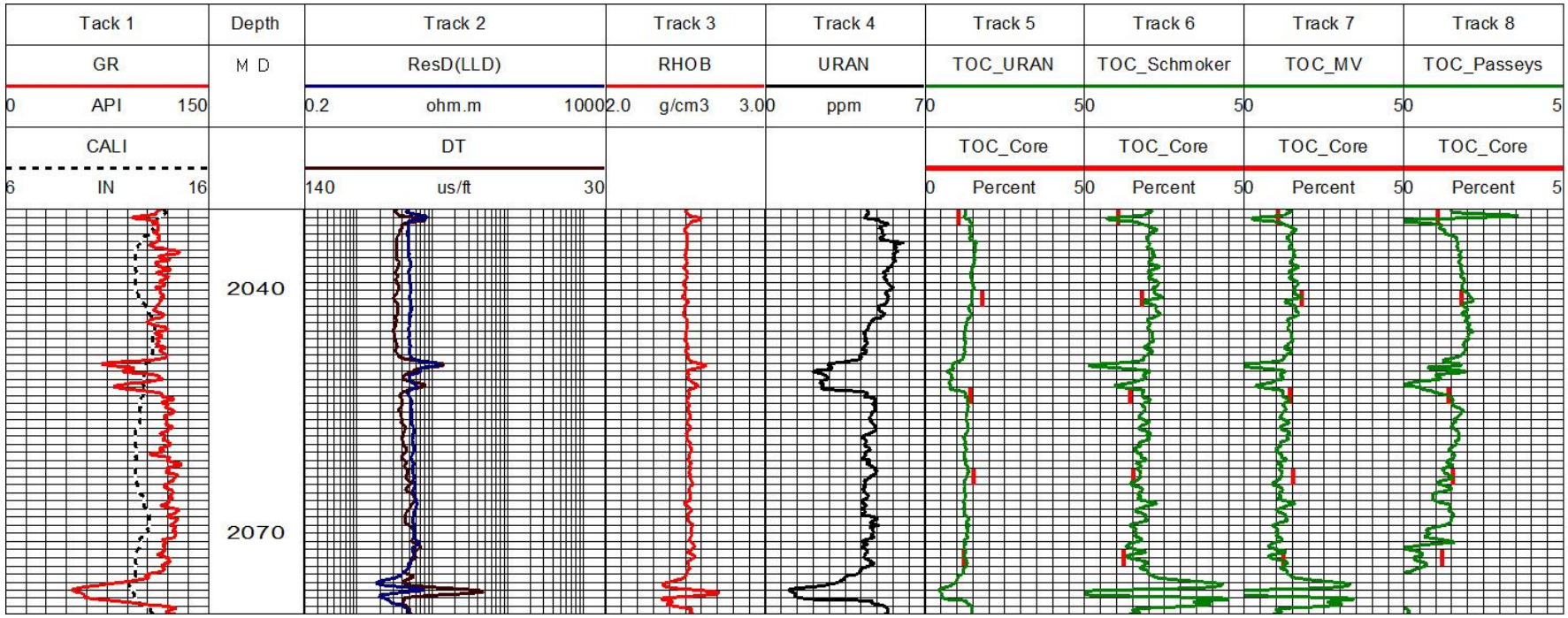

Figure 5.3 TOC estimation of Sembar Formation in Khajar-01 well through selected methods at a depth 2030-2080.

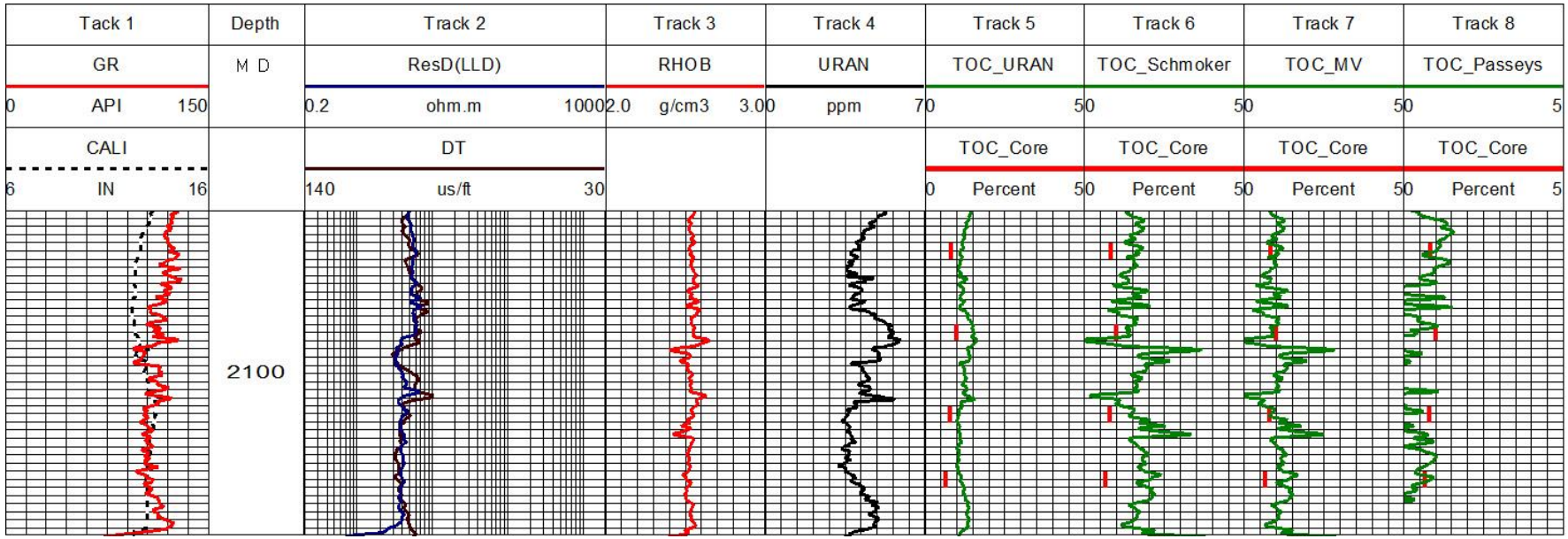

Figure 5.4 TOC estimation of Sembar Formation in Khajar-01 well through selected methods at a depth 2080-2120.

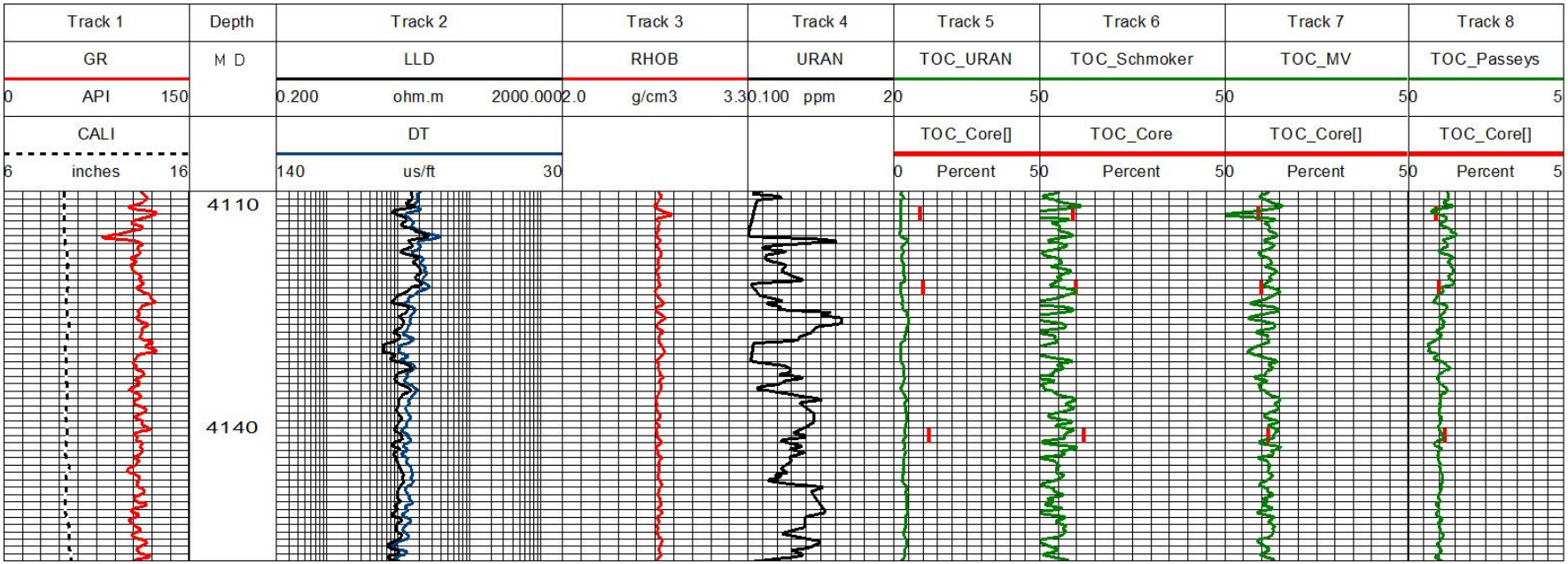

Figure 5.5 TOC estimation of Sembar Formation in Miran-01 well through selected methods at a depth 4108-4158.

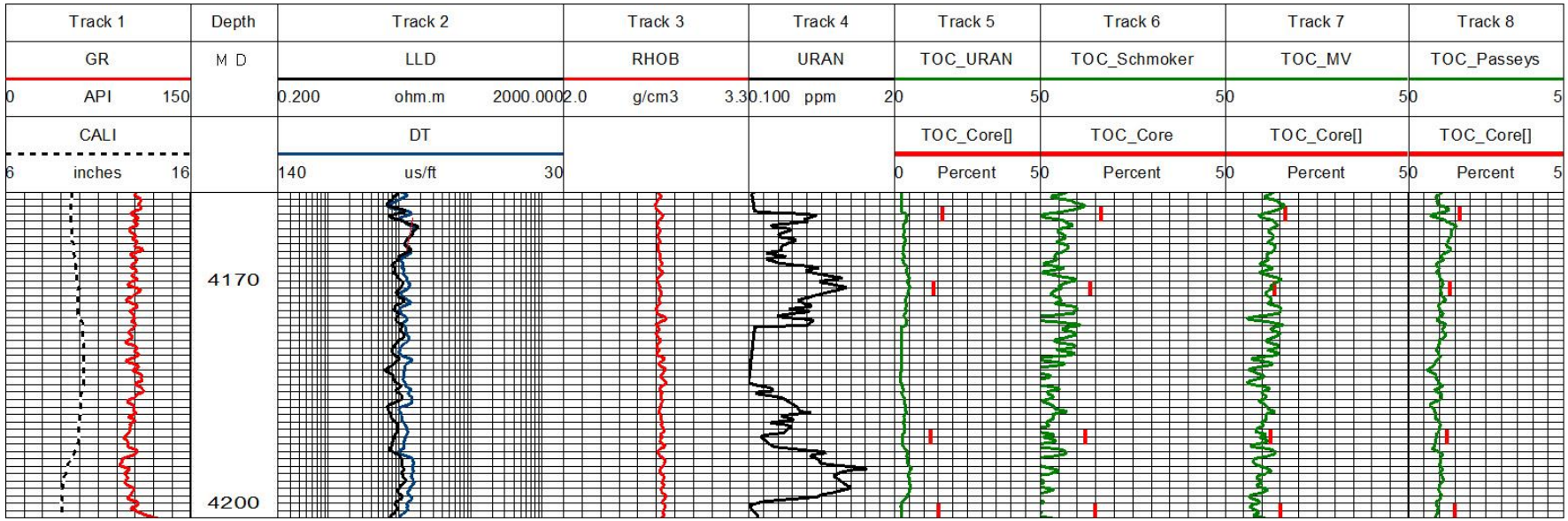

Figure 5.6 TOC estimation of Sembar Formation in Miran-01 well through selected methods at a depth 4158-4202.

Table 5.2 Calculated TOC of Sembar Formation in well Khajari-01.

Khajari-01					
Depth	Cuttings tested TOC	TOC Multivariate fitting Method	TOC Schmoker Method	TOC Fertl and Chilangar Method	TOC Passey Method
1980-82	0.39	1.30	1.9	1.34	0.51
1990-92	0.39	0.50	1.09	0.95	0.47
2010-12	1.37	1.22	1.88	0.82	1.14
2020-22	2.16	1.42	1.97	1.61	1.88
2030-32	1.05	0.71	1.19	1.23	1.15
2040-42	1.80	1.59	2.13	1.41	1.93
2052-54	1.42	1.22	1.80	1.27	1.47
2062-64	1.53	1.15	1.73	1.29	1.52
2072-74	1.21	1.34	1.95	1.25	0.73
2084-86	0.82	1.07	1.69	1.18	0.69
2094-96	0.64	0.79	1.29	1.48	0.90
2104-06	0.98	0.91	1.51	1.01	0.49
2112-14	0.75	1.36	2.01	1.17	0.53
Average	1.12	1.21	1.70	1.23	1.03
Average Difference		-0.09	-0.58	-0.11	0.09

Table 5.3 Calculated TOC of Sembar Formation in well Miran-01.

Miran-01					
Depth	Cuttings tested TOC	TOC Multivariate fitting Method	TOC Schmoker Method	TOC Fertl and Chilangar Method	TOC Passey Method
4110-12	0.90	0.97	0.72	0.24	1.29
4120-22	0.99	1.28	0.65	0.25	1.27
4140-42	1.19	1.27	0.60	0.34	1.13
4160-62	1.65	1.14	0.39	0.37	0.98
4170-72	1.35	1.20	0.47	0.48	1.08
4190-92	1.23	1.07	0.28	0.23	1.01
4200-02	1.50	0.86	0.19	0.27	0.99
Average	1.26	1.11	0.47	0.311	1.12
Average Difference		0.15	0.79	0.95	0.14

Calculated TOC by four methods i-e Schmoker and Hester, Fertl and Chilangar, Multivariate fitting, and Passey method and cuttings tested TOC are shown in the tables 5.1 and 5.2.

CHAPTER 6

CORRELATION

6.1 Background

Correlation coefficient represented by R^2, is a statistic between two variables which shows how strong or weak relationship between these two variables are. These two variables may be two sets of data. There are many types of correlation coefficients exist, each with its own definition and characteristics (Cramer, 2003). Here one set of data is total organic carbon (TOC) from well cuttings tested and the other is calculated TOC from well logs through different methods i-e Schmoker's, Multivariate fitting, Fertl and Chilingar, and Passey's methods. By integration of measured TOC from well cuttings, four cross plots have been drawn for each well as measured TOC verses Schmoker TOC, Measured TOC verses Multivariate fitting TOC, Measured TOC Fertl and Chilingar TOC and Measured TOC verses Passey TOC.

6.2 Correlation of cuttings tested TOC verses Schmoker and Hester calculated TOC

Total Organic Carbon (TOC) of well cuttings analyzed though Carbon/Sulfur Analyzer of two wells, Khajari-01 and Miran-01 have been drawn against bulk density well logs calculated TOC as shown in the figures 6.1 and 6.2. The correlation coefficients between these measured and calculated TOCs values have been calculated which are denoted by R^2. The R^2 value of well Khajari-01 is 0.2878, which is low. R^2 value of well Miran-01 well is 0.5828 which is relatively high as compare to that of Khajari-01 well.

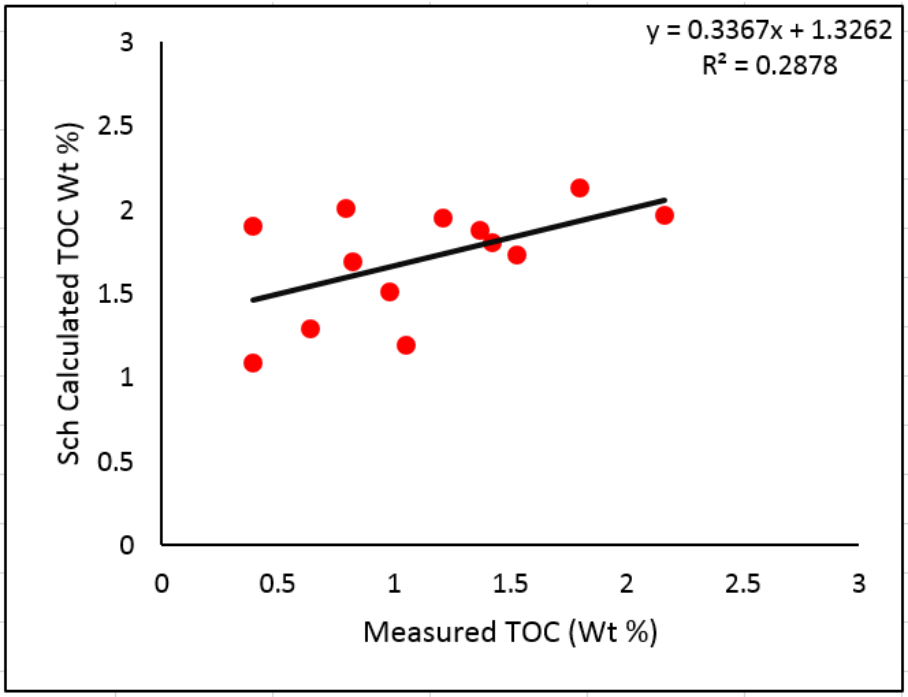

Figure 6.1 Plot of measured TOC verses Schmoker's calculated TOC of Khajari-01 well, showing correlation coefficient.

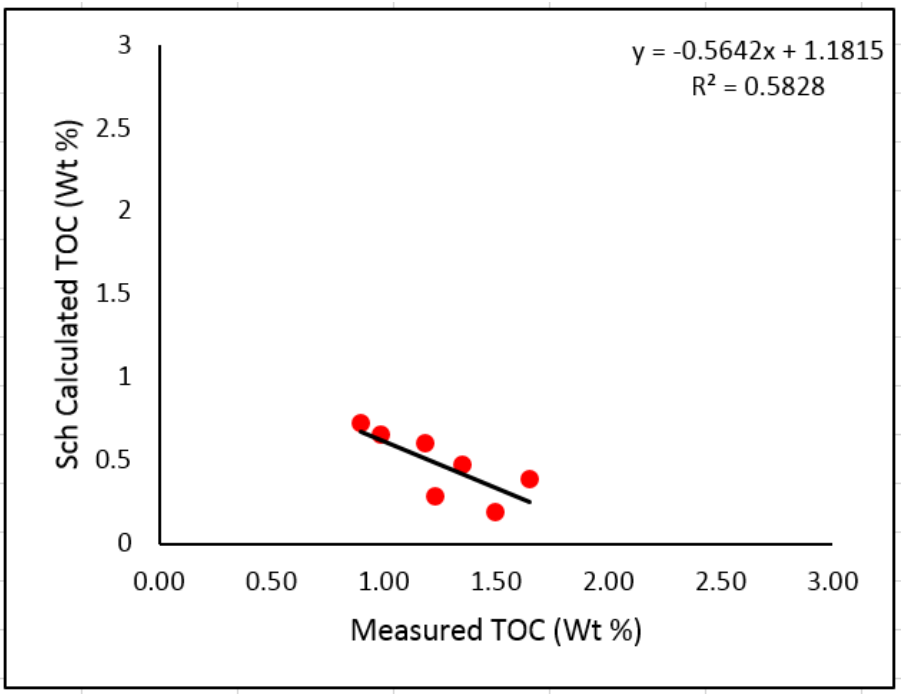

Figure 6.2 Plot of measured TOC verses Schmoker's calculated TOC of Miran-01 well, showing correlation coefficient.

6.3 Correlation of cuttings tested TOC verses Fertl and Chilangar, (1988) calculated TOC

Cuttings tested TOC values have been drawn against Fertl and Chilangar calculated TOC on cross plots for the wells Khajari-01 and Miran-01 as shown in the figures 6.5 and 6.6. Correlation coefficient represented by R^2 has been calculated for both wells. R^2 for the well Khajari-01 is 0.1446 and that of Miran-01 is 0.239. R^2 values for both the wells are very much low, which show that this method is not feasible for calculating TOC in the Sembar Formation.

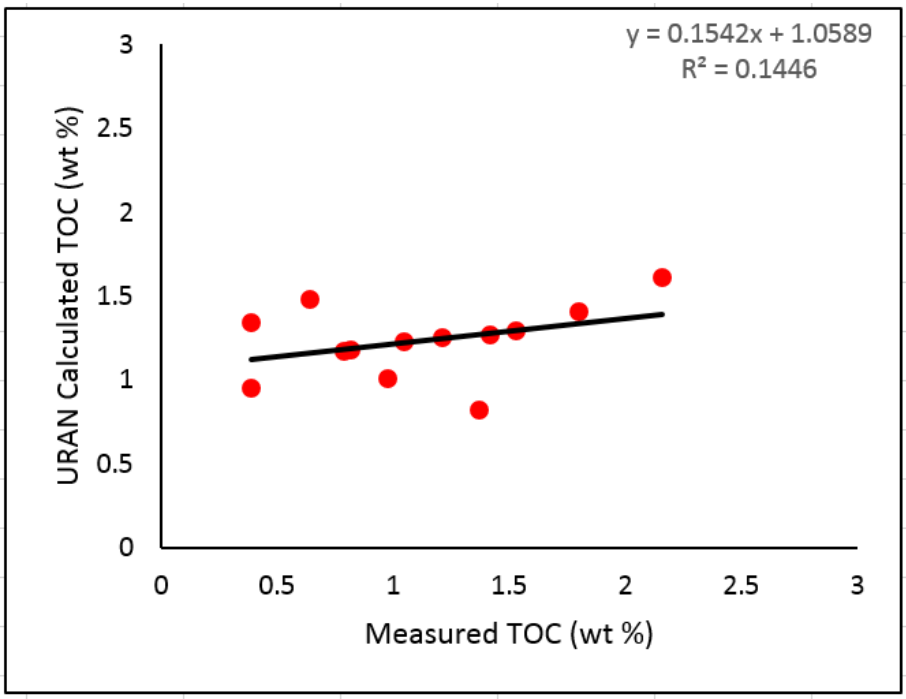

Figure 6.3 Plot of measured TOC verses Fertl and Chilangar calculated TOC of Khajari-01 well, showing correlation coefficient.

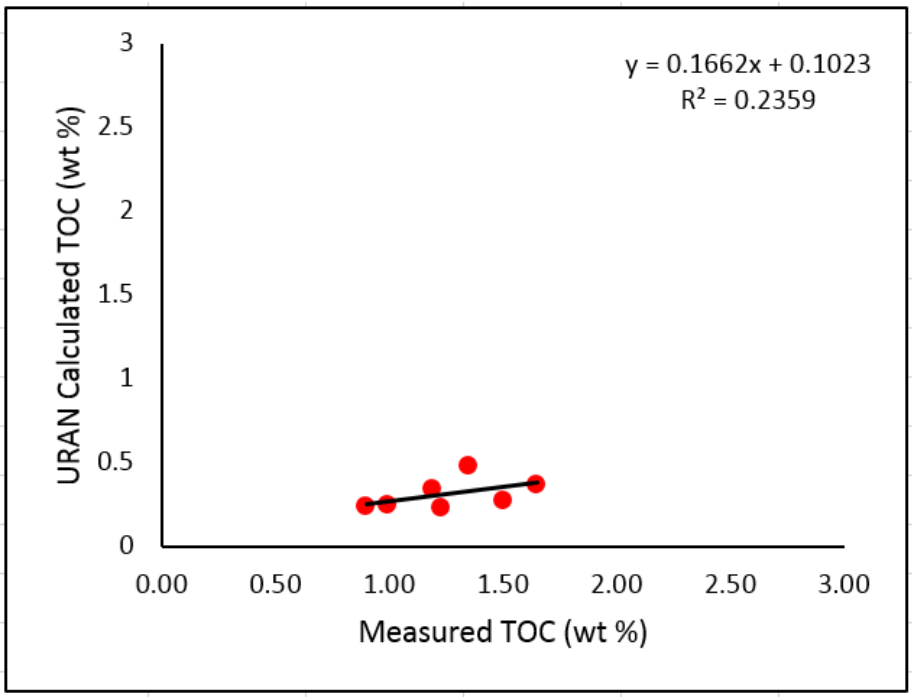

Figure 6.4 Plot of measured TOC verses Fertl and Chilangar calculated TOC of Miran-01 well, showing correlation coefficient.

6.4 Correlation of cuttings tested TOC verses Multivariate fitting calculated TOC

Core TOC measured verses calculated multivariate TOC for the wells Khajari-01 and Miran-01 have been drawn on plots as shown in the figures 5.3 and 5.4. Correlation coefficient for the well Khajari-01 is 0.3556 and that of Miran-01 is 0.0333. R^2 value for Miran-01 is very much low as compare to that of Khajari-01. In fact, R^2 values for both the wells are low and not feasible in practice.

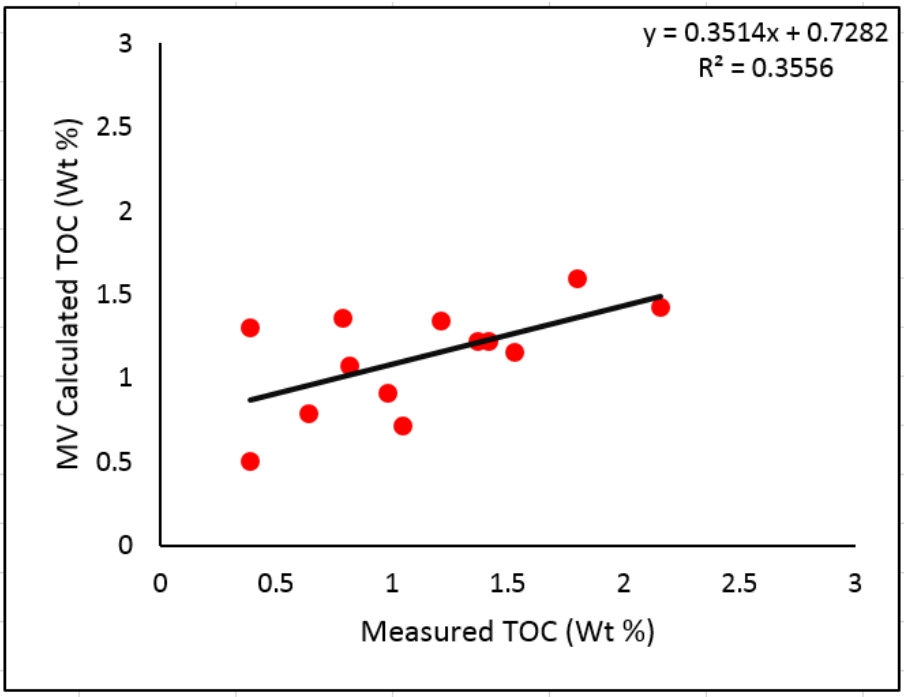

Figure 6.5 Plot of measured TOC verses Multivariate fitting calculated TOC of Khajari-01 well, showing correlation coefficient.

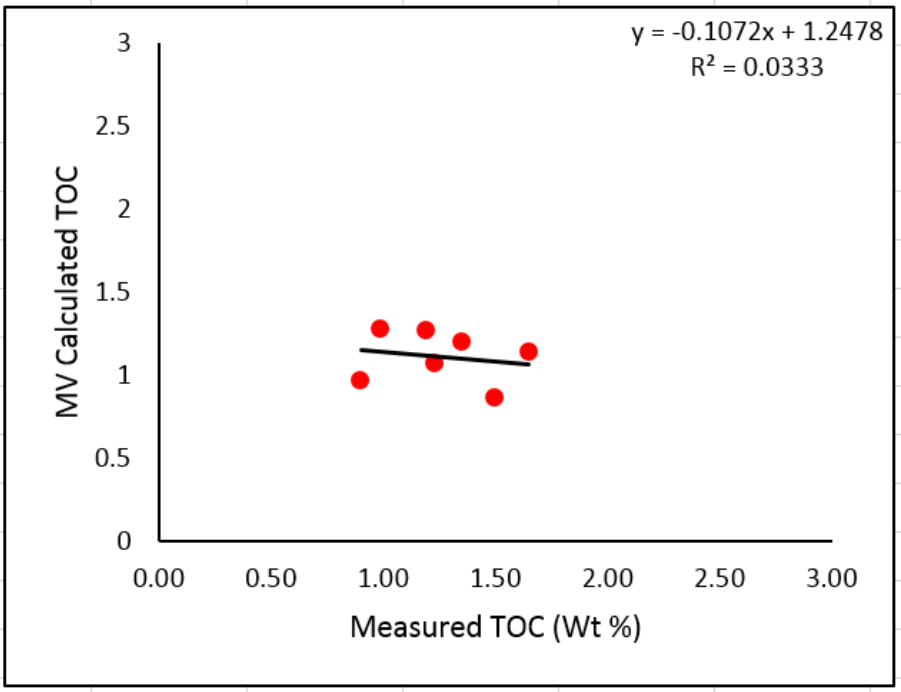

Figure 6.6 Plot of measured TOC verses Multivariate fitting calculated TOC of Miran-01 well, showing correlation coefficient.

6.5 Correlation of cuttings tested TOC verses Passey Method calculated TOC

Cuttings tested TOC measured verses Passey method calculated TOC have been plotted for the wells Khajari-01 and Miran-01 as shown in the figures 6.5 and 6.6. Correlation coefficient values for Khajari-01 well is 0.8018 and that of Miran-01 is 0.8306. R^2 values for both the wells are significantly high. The high correlation coefficient values from Passey method suggest that Passey method is the best fitting method for calculation of total organic carbon content in Sembar Formation.

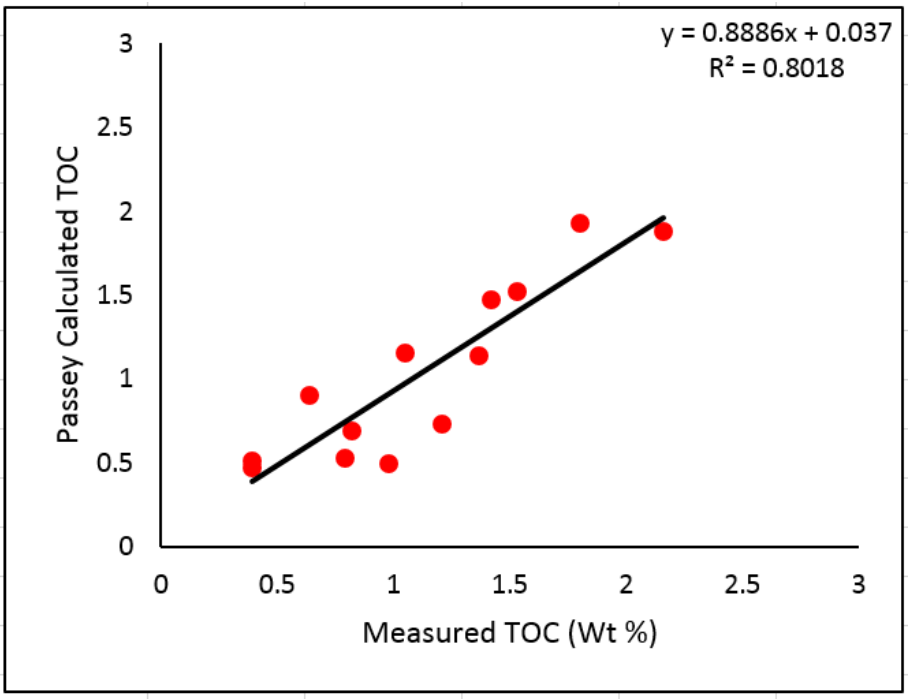

Figure 6.7 Plot of measured TOC verses Passey calculated TOC of Khajari-01 well, showing correlation coefficient.

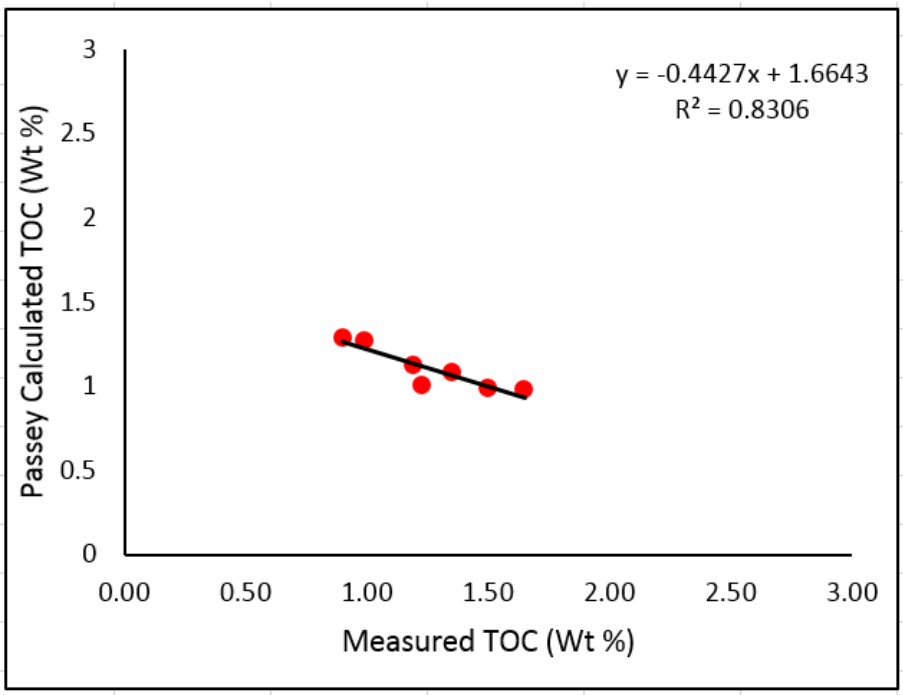

Figure 6.8 Plot of measured TOC verses Passey calculated TOC of Miran-01 well, showing correlation coefficient.

CONCLUSIONS

The geochemical analyses were conducted on 21 rock samples of Sembar Formation to understand the source rock hydrocarbon generation potential from two wells in the Lower Southern Indus Basin, Pakistan. Additionally, complete suites of well logs of these two wells were collected for estimation of TOC through well logs. Results reveal that:

i. Van-Krevelen and Langford diagrams indicate that Sembar Formation of Khajari-01 well is gas prone while that of Miran-01 is non-productive.

ii. Sembar Formation in Khajari-01 well has poor to very good organic richness and Miran-01 is fair to good, while in terms of petroleum potential both wells have poor potential yield.

iii. Samples from Khajari-01 well in terms of generation potential falls in the range of poor to excellent source rock while that of Miran-01 is fair to good source rock.

iv. In terms of Tmax and Production Index, Sembar Formation in Khajari-01 well is immature to early mature, while Miran-01 appears over mature.

v. Natural gamma-ray spectroscopy method for TOC estimation has been applied to Sembar Formation in the wells Khajari-01 and Miran-01 which has poor correlation coefficient values of 0.1446 and 0.239 with well cuttings tested TOC.

vi. Schmoker and Hester's method have also been applied to the same formation in both wells, which gives a relatively high R^2 value i-e 0.2878 and 0.5828, but still, these values are not reliable.

vii. Multivariate Fitting method has also been applied to Sembar Formation in the well Khajari-01 and Miran-01, which gives poor values of correlation coefficient, 0.3556 and 0.0333 making it unreliable for calculation of TOC through well logs.

viii. Passey method has been applied which gives high R^2 values of 0.8018 in well Khajari-01 and 0.8306 in well Miran-01. As compared to the other three methods, Passey method of TOC calculation from well logs is more reliable.

REFERENCES

Ahmad, N., Ahsan, N., Sameeni, S.J., Mirag, M.A.F. and Khan, B., 2013. Sedimentology and reservoir potential of the lower Eocene Sakesar limestone of Dandot Area, Eastern Salt Range, District Chakwal, Pakistan. Science International (Labor), 25(3): 521-529.

Alshakhs, M. and Rezaee, M.R., 2017. A new method to estimate total organic carbon (TOC) Content, an example from Goldwyer Shale Formation, the Canning Basin. The Open Petroleum Engineering Journal, 10: 118-133.

Bender, F. and Raza, H.A., 1995. Geology of Pakistan.

Baskin, D.K., 1997. Atomic H/C ratio of kerogen as an estimate of thermal maturity and organic matter conversion. AAPG bulletin, 81(9): 1437-1450.

Clementz, D.M., 1979. Effect of oil and bitumen saturation on source-rock pyrolysis: Geologic notes. AAPG Bulletin, 63(12): 2227-2232.

Crain, E.R., 2006. Crain's Petrophysical Pocket Pal. Ontario: ER Ross.

Espitalie, J., Deroo, G. and Marquis, F., 1985. Rock-Eval pyrolysis and its applications. Revue De L Institut Francais Du Petrole, 40(5): 563-579.

Duroy, Y., Farah, A. and Lillie, R.J., 1989. Reinterpretation of the gravity field in the Himalayan foreland of Pakistan. Tectonics of the Western Himalayas Geol. Soc. Am, 132: 217-236.

EIA, U., 2013. Annual energy outlook 2013. US Energy Information Administration, Washington, DC: 60-62.

Farah, A., Abbas, G., De Jong, K.A. and Lawrence, R.D., 1984. Evolution of the lithosphere in Pakistan. Tectonophysics, 105(1-4): 207-227.

Fatmi, A.N., 1977. Mesozoic. Stratigraphy of Pakistan, 1: 29-56.

Gonzalez, J., Lewis, R., Hemingway, J., Grau, J., Rylander, E. and Pirie, I., 2013, August. Determination of formation organic carbon content using a new neutron-induced gamma ray spectroscopy service that directly measures carbon. In Unconventional Resources Technology Conference (1100-1109). Society of

Exploration Geophysicists, American Association of Petroleum Geologists, Society of Petroleum Engineers.

Huang, R., Wang, Y., Cheng, S., Liu, S. and Cheng, L., 2015. Selection of logging-based TOC calculation methods for shale reservoirs: A case study of the Jiaoshiba shale gas field in the Sichuan Basin. Natural Gas Industry B, 2(2-3): 155-161.

Jadoon, I.A., Lawrence, R.D. and Hassan, K.S., 1994. Mari-Bugti pop-up zone in the central Sulaiman fold belt, Pakistan. Journal of Structural Geology, 16(2): 147-158.

Jadoon, I.A., Lawrence, R.D. and Lillie, R.J., 1994. Seismic data, geometry, evolution, and shortening in the active Sulaiman fold-and-thrust belt of Pakistan, southwest of the Himalayas. AAPG bulletin, 78(5): 758-774.

Kadri, I.B., 1995. Petroleum geology of Pakistan. Pakistan Petroleum Limited.

Kazmi, A.H. and Jan, M.Q., 1997. Geology and tectonics of Pakistan. Graphic publishers.

Lashin, A. and Mogren, S., 2012. Total organic carbon enrichment and source rock evaluation of the Lower Miocene rocks based on well logs: October oil field, Gulf of Suez-Egypt. Int J Geosci, 3: 683-695.

Langford, F.F. and Blanc-Valleron, M.M., 1990. Interpreting Rock-Eval pyrolysis data using graphs of pyrolizable hydrocarbons vs. total organic carbon (1). AAPG Bulletin, 74(6): 799-804.

Mohammednoor, M. and Orhan, H., 2017. Organic geochemical characteristics and source rock potential of upper pliocene shales in the akcalar lignite basin, turkey. Oil Shale, 34(4).

Molnar, P., Atwater, T., Mammerickx, J. and Smith, S.M., 1975. Magnetic anomalies, bathymetry and the tectonic evolution of the South Pacific since the Late Cretaceous. Geophysical Journal International, 40(3): 383-420.

Nazeer, A., Solangi, S.H., Brohi, I.A., Usmani, P., Napar, L.D., Jhangir, M., Hameed, S. and Manshoor, S.M., 2012. Hydrocarbon potential of zinda pir anticline,

eastern Sulaiman fold belt, middle Indus Basin, Pakistan. Pakistan Journal of Hydrocarbon Research, 22: 124-138.

Passey, Q.R., Creaney, S., Kulla, J.B., Moretti, F.J. and Stroud, J.D., 1990. A practical model for organic richness from porosity and resistivity logs. AAPG bulletin, 74(12): 1777-1794.

Patriat, P. and Achache, J., 1984. India–Eurasia collision chronology has implications for crustal shortening and driving mechanism of plates. Nature, 311(5987): 615.

Peters, K.E. and Cassa, M.R., 1994. Applied source rock geochemistry: Chapter 5: Part II. Essential elements.

Pilbeam, D., Meyer, G.E., Badgley, C., Rose, M.D., Pickford, M.H., Behrensmeyer, A.K. and Shah, S.I., 1977. New hominoid primates from the Siwaliks of Pakistan and their bearing on hominoid evolution. Nature, 270(5639): 689.

Pilbeam, D., Barry, J., Meyer, G.E., Shah, S.I., Pickford, M.H., Bishop, W.W., Thomas, H. and Jacobs, L.L., 1977. Geology and palaeontology of Neogene strata of Pakistan. Nature, 270(5639): 684.

Powell, T.G. and Snowdon, L.R., 1979. Geochemistry of crude oils and condensates from the Scotian Basin, offshore eastern Canada. Bulletin of Canadian Petroleum Geology, 27(4): 453-466.

Sclater, J.G. and Fisher, R.L., 1974. Evolution of the east: Central Indian Ocean, with emphasis on the tectonic setting of the Ninetyeast Ridge. Geological Society of America Bulletin, 85(5): 683-702.

Searle, M.P., 1983. Stratigraphy, structure and evolution of the Tibetan–Tethys zone in Zanskar and the Indus suture zone in the Ladakh Himalaya. Earth and Environmental Science Transactions of The Royal Society of Edinburgh, 73(4): 205-219.

Sheikh, N. and Giao, P.H., 2017. Evaluation of shale gas potential in the Lower Cretaceous Sembar Formation, the Southern Indus Basin, Pakistan. Journal of Natural Gas Science and Engineering, 44: 162-176.

Shah, S.K., 1991. Stratigraphic setting of the Phanerozoic rocks along the northern boundary of the Indian plate. Physics and Chemistry of the Earth, 18: 317-328.

Schmoker, J.W., 1979. Determination of organic content of Appalachian Devonian shales from formation-density logs: Geologic notes. AAPG Bulletin, 63(9): 1504-1509.

Sun, S.Z., Sun, Y., Sun, C., Liu, L. and Dong, N., 2013. Method of calculating total organic carbon from well logs and its application on rock's properties analysis. Integration Geo Convention 2013, Geoscience Engineering Partnership.

Tissot, B.P. and Welte, D.H., 1984. Petroleum Formation and Occurrence, 2nd edn, 699.

Tissot, B.P. and Welte, D.H., 1984. Petroleum Formation and Occurrence, 2nd edn, 699.

Viqar-un-nisa Quadri, S.M., 1986. Hydrocarbon prospects of southern Indus basin, Pakistan. AAPG Bulletin, 70(6): 730-747.

Van Krevelen, D.W., 1984. Organic geochemistry—old and new. Organic Geochemistry: 1-10.

Wandrey, C.J., Law, B.E. and Shah, H.A., 2004. Sembar Goru/Ghazij composite total petroleum system, Indus and Sulaiman-Kirthar geologic provinces, Pakistan and India (No. 2208-C).

Williams, M.D., 1959, January. 19. Stratigraphy of the Lower Indus Basin, West Pakistan. In 5th World Petroleum Congress. World Petroleum Congress.

Zaigham, N.A. and Mallick, K.A., 2000. Prospect of hydrocarbon associated with fossil-rift structures of the southern Indus basin, Pakistan. AAPG bulletin, 84(11): 1833-1848.